(11) **EP 1 772 588 A2**

(12) EUROPEAN PATENT APPLICATION

(43) Date of publication:

11.04.2007 Bulletin 2007/15

(51) Int Cl.:

E06C 5/44 (2006.01)

E06C 5/04 (2006.01)

(21) Application number: 06119983.2

(22) Date of filing: 01.09.2006

(84) Designated Contracting States:

AT BE BG CH CY CZ DE DK EE ES FI FR GB GR HU IE IS IT LI LT LU LV MC NL PL PT RO SE SI SK TR

Designated Extension States:

AL BA HR MK YU

Fig.1

(30) Priority: 08.09.2005 DE 102005042721

(71) Applicant: IVECO MAGIRUS AG D-89079 Ulm (DE)

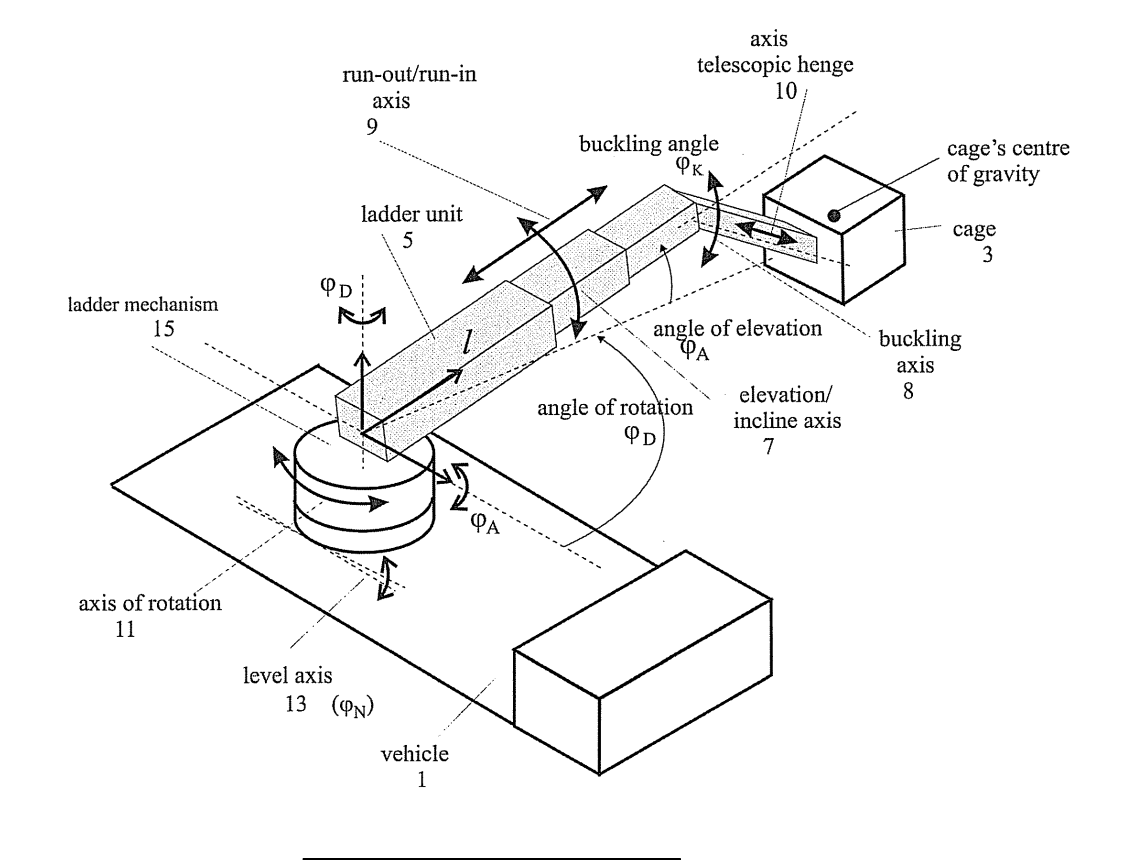
(72) Inventor: Sawodny, Oliver 70186, Stuttgart (DE)

(74) Representative: Borsano, Corrado Notarbartolo & Gervasi S.p.A. Corso di Porta Vittoria, 9 20122 Milano (IT)

(54) Articulated ladder or raisable platform with position path control and active vibration damping

(57) Turntable ladder or the like, with a telescopic ladder unit and, attached at the end of the ladder unit, an articulated arm which carries a cage, which turntable ladder contains a control for moving the ladder sections, formed in such a way that, during cage travel, vibrations of the ladder sections are suppressed, while at least one of the measured variables, bending of the ladder unit in the horizontal and vertical direction, angle of elevation,

angle of rotation, run-out length and torsion of the ladder unit is fed back via a controller to the control variables for the drives and for which a pilot control is provided which represents the idealised movement behaviour of the ladder during cage travel in a dynamic model, based on differential equations and calculates the idealised control variables for the ladder section drives from the dynamic model for an essentially vibration-free movement of the ladder.



Description

Field of the Invention

[0001] The invention concerns a turntable ladder or the like, with a telescopic ladder unit and, attached at the end of the ladder unit, an articulated arm which carries a cage.

Prior Art

20

30

35

40

45

50

[0002] Turntable ladders, for example fire brigade ladders or similar devices, such as articulated or telescopic mast platforms and hoist rescue devices, are generally mounted on a vehicle so that they can be rotated or elevated. In the special case of an articulated ladder, an inclinable articulated arm is additionally provided which can, furthermore, with another axis, be telescopic. The control is a position path control which maintains the cage or platform on a specified position path in the working area of the turntable ladder or raisable platform. Vibrations and oscillatory movements of the cage or hoist platform are thereby actively damped.

[0003] The German patent specifications DE 100 16 136 C2 and DE 100 16 137 C2 each disclose turntable ladders which are provided with command or control for moving the ladder sections. According to DE 100 16 136 C2, vibrations of the ladder sections are prevented by feeding back at least one of the measured variables: bending of the ladder in the horizontal and vertical direction, angle of elevation of the ladder, angle of rotation, run-out length and cage mass, via a controller to the control variables for the drives. A pilot control reproduces the idealised motion behaviour of the ladder in a dynamic model, based on differential equations, and calculates idealised control variables for the drives of the ladder sections, in order to enable an essentially vibration-free movement of the ladder.

[0004] Such turntable ladders are controlled hydraulically or electro-hydraulically by hand levers. In the case of a purely hydraulic control, the hand lever deflection is directly converted by the hydraulic control circuit into a proportional control signal for the control block designed as a proportional valve. Damping elements in the hydraulic control circuit can be used to make the movements less jerky and smoother in transition. However, these cannot be satisfactorily adapted to the entire operating range of run-out lengths and angles of elevation. Furthermore, this often leads to highly damped positions with sluggish response behaviour.

[0005] In the signal flow, the electro-hydraulic controls firstly convert the hand lever deflection into an electrical signal which is further processed in a control device with a microprocessor. Thereby, the signal, according to state of the art, is damped by ramp functions so that movements of the turntable ladder or working platform are less jerky and smoother. The processed electrical signal is then passed to the hydraulic proportional valve. The slope of the ramp function limits the damping effect and is a measure of the response behaviour.

[0006] Whereas the damping of vibration or oscillatory movements of conventional simple turntable ladders, which carry the cage at the end of their telescopic ladder unit, is satisfactorily possible by means of the control described above, the vibration-free guidance of turntable ladders with an articulated arm at the end of a telescopic ladder unit, which can moreover be telescopic itself, causes significant problems as, in this case, further degrees of freedom and vibration components must be considered. This is beyond the capabilities of known command and control systems, according to the state of the art, so that the entire ladder system can degrade into critical operating states in deployment, which can lead to dangerous situations.

Summary of the Invention

[0007] The objective of the invention is to equip a turntable ladder, having an articulated arm, with a position path control which actively damps vibrations which occur (either during movement or in the static position, e.g. through wind effects or loading changes) or guides the cage or working platform on a specified position path.

[0008] This objective is achieved according to the invention by means of a turntable ladder having an articulated arm or telescopic arm or the like with a position path control or active vibration damping according to Claim 1.

[0009] Preferable embodiments of the turntable ladder according to the invention result from the subclaims.

[0010] The attached claims are considered an integral part of the present description.

[0011] The position path control with active vibration damping is based on the principle of describing the dynamic behaviour of the mechanical and hydraulic systems of the turntable ladder firstly as a dynamic model based on differential equations.

[0012] Based on this dynamic model, a pilot control can be designed which, under the idealised conditions of the dynamic model, generates no vibrations of the ladder unit when moving the axes of the articulated ladder and guides the cage exactly on the specified position path. Unlike simple turntable ladders, on account of the retracted articulated arm, additional torsional vibrations occur in the case of articulated ladders, which also have to be damped by the rotary actuation. Furthermore, the telescopic axis of the articulated arm has to be taken into account. These additional axes

must be considered in the position path planner.

[0013] The prerequisite for the pilot control is firstly the generation of the position path in the working area which has to be undertaken by the position path planning module. The position path planning module generates the position path which is given to the pilot control in the form of time functions for the cage position, velocity and acceleration, the jerking and, if necessary, the time derivative of the jerking, from the input requirement of the reference velocity proportional to the deflection of the hand lever in the case of semi-automatic operation or target points in the case of fully automatic operation.

[0014] As, nevertheless, vibrations or deviations from the reference position path can arise, the system of pilot control and position path planning module is supported by a state controller during strong deviations from the idealised dynamic model (e.g. through disturbance). This feeds back at least one of the measured variables: angle of elevation, run-out length, angle of rotation, articulation angle, bending of the ladder in the horizontal and vertical direction or torsion respectively.

Brief Description of the Drawings

15

20

25

35

50

[0015] The invention will be exemplified below with the aid of the drawings, in which:

- Fig. 1 shows the basic mechanical structure of a turntable ladder by way of example
- Fig. 2 shows rigid and elastic degrees of freedom of the system
- Fig. 3 shows interaction of hydraulic control and position path control
- Fig. 4 shows the entire structure of the position path control
- Fig. 5 shows the semi-automatic and fully automatic operation of the position path planning module
- Fig. 6 shows modelling as a system with equivalent masses and spring damper elements
- Fig. 7 shows the structure of the axis controller for the axis of rotation
- Fig. 8 shows the axis controller for the axis of elevation/inclination
- Fig. 9 shows kinematics for the axis of elevation.

Detailed Description of the Invention

[0016] Fig. 1 shows the basic mechanical structure of a turntable ladder with articulated arm or the like. The turntable ladder is generally mounted on a vehicle 1. To position the cage 3 in the working area, the ladder unit 5 can be tilted with the elevation/inclination axis 7 by the angle φ_A and folded with the articulation axis 8 by the angle φ_K . The articulated arm can be extended and retracted with the telescopic articulated arm axis 10. The ladder length *I* can be varied with the run-out/run-in axis 9. The rotation axis 11 allows orientation by the angle φ_D about the vertical axis. In the case of a vehicle which is not standing horizontally, an undesirable additional inclination can be compensated with the level axis 13 upon rotation of the ladder unit by tilting the ladder mechanism 15 by the angle φ_N .

[0017] Fig. 2 shows once more separately the rigid and elastic degrees of freedom of the system relevant for the derivation of the dynamic model. The rigid degrees of freedom φ_A , φ_K , φ_D , I, I_K correspond to the 5 main ladder axes (without level axis). The elastic degrees of freedom are the horizontal and vertical bending v_x , v_y , as well as the torsion of the ladder unit α_X and the horizontal and vertical bending w_x , w_y as well as the torsion β_X of the articulated arm.

[0018] Generally, the turntable ladder has a hydraulic drive system 21. It consists of the hydraulic pump 33 driven by the drive motor, the proportional valve 39 and the hydraulic motors 311 and hydraulic cylinders 313. The hydraulic control is generally equipped with systems with auxiliary flow rate control for the hydraulic circuits with load-sensing properties. It is essential in this case that the control voltages u_{StD} , u_{StA} , u_{StN} , u_{StE} u_{StK} , u_{StT} at the proportional valves are converted by the auxiliary flow rate control into proportional flow rates Q_{FD} , Q_{FA} , Q_{FN} , Q_{FE} , Q_{FK} , Q_{FT} in the corresponding hydraulic circuit (Fig. 3).

[0019] It is essential that the time functions for the control voltages of the proportional valves are no longer derived directly from the hand levers, for example by ramp functions, but are calculated in the position path control 31 in such a way that no vibrations occur when the ladder is moved and the cage follows the desired position path in the working area. [0020] The basis for this is a dynamic model of the turntable ladder system with the aid of which this object is achieved based on the sensor data of at least one of the variables v_y , v_z , α_x , l, φ_A , φ_D , φ_{N} , φ_{K} , l_K and the command inputs $\dot{q}_{Ziel} = [\dot{\varphi}_{DZiel},\dot{\varphi}_{AZiel},\dot{l}_{Ziel},\dot{$

ordinate, to the angle of elevation co-ordinate, to the angle of articulation co-ordinate and to the run-out length and their derivatives are calculated from these pre-set variables in the position path planning module 39 or 41 (Fig. 4), as explained in detail below.

[0021] Firstly, the entire structure (Fig. 4) of the position path control 31 will be explained below.

20

30

35

50

[0022] The function of the position path planning module 39 or 41 is the calculation of the time functions of the reference cage position, of the rotation, elevation, run-out, telescopic and articulation axes and their derivatives which are combined in the vectors Φ_{Dref} , Φ_{Aref} , Φ_{Kref} , Φ_{Kref} . Each of these vectors comprises at most 4 components up to the 3rd derivative (position, velocity, acceleration, jerking). The reference position vectors are fed to the axis controllers 43, 45, 47, 49, 411 and 413 which hence calculate the control functions u_{StD} , u_{StA} , u_{StE} , u_{StT} , u_{StN} , u_{StK} for the proportional valves 39 of the hydraulic drive system 21 by evaluating at least one of the sensor values v_{v} , v_{x} , α_{x} , l_{x} , q_{x} , q_{D} , q_{D} , q_{N} , q_{K} .

[0023] The operator pre-selects the target speeds or the destinations either via the hand lever 35 at the operating panels (semi-automatic operation) or via a target point matrix 37 which has been stored in the computer during a previous turntable ladder run (fully automatic operation). By taking into account the kinematic restrictions (maximum velocity and maximum acceleration), the semi-automatic position path planning module (41) calculates the corresponding time functions of the reference cage position from the hand lever signals for the various directions of movement (rotation, elevation/inclination, run-in/run-out and articulation of the articulated arm) which can be taken as the target velocity for the respective axis. As the kinematic restrictions (especially the maximum velocity for each axis) are not constant, but can vary, for example depending on the run-out length or the mass in the cage, position path planning methods which calculate in advance the entire position path to be followed are not suitable for the present application. The aim of fully automatic operation is to move along a previously travelled position path as quickly as possible (possibly slowly for the purpose of avoiding collisions with obstacles) while maintaining a previously defined maximum allowed deviation. A calculation of the time function by the steepness limiter 53 is adequate for semi-automatic operation. For fully automatic operation, the steepness limiter 53 is supplemented by a positioning loop with a proportional controller (p-controller) with variable limitation 57 (Fig. 5).

[0024] The difference between the target position and actual corrected reference position is amplified by the p-controller and limited to the maximum allowed velocity $\dot{\phi}_{Dmax}$. The output of the additional feedback is then the corresponding target velocity $\dot{\phi}_{Dziel}$, which in turn forms the input of the steepness limiter 53 of the semi-automatic position path planning module (41). In order to allow for altered kinematic limitations, the maximum velocity for each axis can be changed proportionally by a factor, as the limitation is variable as a function of the maximum velocity. This factor can also be use for the synchronisation of the axes and is calculated in the module 'calculation of synchronisation factors' 51.

[0025] The calculation of the axis synchronisation is carried out taking into account the distance to the next target point in the target point matrix. The axis requiring the longest time to reach the next target point limits the movement. This means that the proportional factor for the axis which has to cover the longest position path to the next target point is equal to 1. The corresponding target velocity is thus equal to the maximum velocity. Moreover, the velocities of the other axes reduce proportionally.

[0026] The transfer to the next target point of the respective axis in the target point matrix is dependent upon the remaining distance from the actual position of the ladder to the actual target point and the maximum deviation which can occur if the next target point in the target point matrix is used as actual target position. For this the actual ladder position is first of all converted into Cartesian co-ordinates in the co-ordinate transformation module 55. As prerequisite for subsequent switching/changing to the next target point, the Euclidean distance to the next target point and the distance in the normal direction of a straight line from the actual position of the ladder to the next but one target position are then calculated 59. Switching occurs if both distances lie within a specified limit. The ladder thus remains within a defined corridor while travelling.

[0027] The time functions for the reference position of the cage in all relevant directions of motion with the mentioned derivatives are thereby available at the output of the semi-automatic position path planner as well as the fully automatic position path planner, taking into account the kinematic restrictions.

[0028] The time functions are fed to the respective axis controllers, whose structure is described below.

[0029] The output functions of the position path planning module are fed to the corresponding pilot control blocks in the form of reference cage position in the individual directions as well as their derivatives (velocity, acceleration, jerking and derivative of jerking). The functions are amplified in these blocks in such a way that, as a result, position path-true travel of the ladder without vibrations ensues under the idealised assumptions/conditions of the dynamic model. The basis for the determination of the pilot control gains is the dynamic model which will be derived for the individual axes in the following sections. Under these idealised conditions, the vibration of the turntable ladder is thereby eliminated and the cage follows the generated position path.

[0030] As, however, disturbance such as wind effects can affect the turntable ladder and the idealised model can only partially reproduce the existing dynamic circumstances, the pilot controls can be supplemented by corresponding state controller blocks. The measured variables for the respective positions as well as for the bending and torsion of the ladder unit (and optionally their derivatives) are amplified in these blocks and fed back again to the servo input The derivatives

of the measured variables are generated numerically in the microprocessor control.

[0031] The derivation of the dynamic model, which is the basis for the calculation of the pilot control gains and the state controller, should now serve to explain the procedure in detail.

[0032] The model is derived as a multiple body system with springs and damper elements via the Lagrange formalism. A turntable ladder or the like is considered exemplary as multiple axis manipulator with three rotational as well as one linear degrees of freedom. In addition to these rigid degrees of freedom, the movements of the elastic degrees of freedom in the articulated arm and ladder unit (bending in the longitudinal and transverse direction as well as torsion about the longitudinal axis) are taken into account in the model. In summary, the rigid degrees of freedom listed as follows result for the creation of the model (Fig. 6):

10

 φ_A : Angle of elevation φ_D : Angle of rotation φ_K : Articulation angle I_A : Length of ladder unit

15

20

as well as the following elastic degrees of freedom (Fig. 6):

 α_{v} : Torsion of the ladder unit

 $\textit{v}_{\textit{v}}$: Bending of the ladder unit in the horizontal direction

 v_z : Bending of the ladder unit in the vertical direction

 β_x : Torsion of the articulated arm

25

30

 w_v : Bending of the articulated arm in the horizontal direction

 w_z : Bending of the articulated arm in the vertical direction

[0033] In the creation of the model, the turntable ladder or the like is not regarded as a system of large elements. By calculating the equivalent masses and equivalent moments of inertia, the entire system can be regarded as a system consisting of three point masses. The system elements are thereby approximated by three equivalent masses and the elastic degrees of freedom considered as spring damper elements (see Fig. 6). By the method of 2nd order Lagrange equations, one obtains ten mutually independent differential equations with a total of ten degrees of freedom of the system. Represented in matrix form, this results in:

40

45

35

$$\underline{M}\underline{\ddot{q}} + \underline{D}\underline{\dot{q}} + \underline{C}[\underline{\dot{q}},\underline{q}] + \underline{K}\underline{q} + \underline{G}[\underline{q}] = \underline{F}$$
 (10)

M: Mass matrix

D: Damping matrix

C: Coriolis and centripetal vector

K: Stiffness vector

G: Gravitation vector

F: Vector of external forces

50 [0034] The generalised forces F on the right-hand side of the equation of motion are the moments or forces applied by the hydraulic drives. The equation of motion (Equ. 11) is simplified in the following way. The displacement of the centres of gravity of the part bodies results exclusively from movements in the rigid co-ordinates, whereby the displacements in bending and torsion in the elements of the mass matrix can be set to zero. The elastic degrees of freedom belonging to the articulated arm can be neglected owing to the high bending and torsion stiffness of the articulated arm.
These two assumptions result in a reduction in the dimensions of the system from ten to seven degrees of freedom. The elements of the individual equations of motion of Equ. 10 can be determined by using symbolic methods available in commercial computer algebra systems. The simplified structure of the mass matrix of the equations of motion (Equ. 10) results in:

$$\underline{M}\underline{\ddot{q}} = \begin{bmatrix}
m_{11} & 0 & 0 & \underline{0} & \underline{m}_{15} & \underline{m}_{16} & 0 & \overline{\phi}_{\underline{D}} \\
0 & m_{22} & \underline{m}_{23} & m_{24} & 0 & 0 & m_{27} & \overline{\phi}_{A} \\
0 & m_{32} & \underline{m}_{33} & m_{34} & 0 & 0 & m_{37} & \overline{\phi}_{S} \\
0 & m_{42} & \underline{m}_{43} & \underline{m}_{44} & 0 & 0 & 0 & \overline{l}_{A} \\
m_{51} & 0 & \overline{0} & \overline{0} & \overline{m}_{55} & \overline{m}_{56} & \overline{0} & \overline{\alpha}_{x} \\
m_{61} & 0 & 0 & 0 & \underline{m}_{65} & \underline{m}_{66} & 0 & \overline{v}_{y} \\
0 & m_{72} & \underline{m}_{73} & \overline{0} & 0 & 0 & \underline{m}_{77} & \overline{v}_{z}
\end{bmatrix} \tag{11}$$

[0035] Two groups of differential equations can be extracted from Equ. 11, each of which can be summarised in a subsystem. The rows marked by a single dashed line show the subsystem rotation and the rows marked by a dotted line show the subsystem elevation/inclination. With the implemented simplification one obtains the following structure for the other matrices of the equation of motion:

Damping matrix:

5

15

20

40

$$\underline{D}\underline{\dot{q}} = \begin{bmatrix}
d_{11} & 0 & 0 & 0 & 0 & 0 & 0 \\
0 & d_{22} & 0 & 0 & 0 & 0 & 0 \\
0 & 0 & d_{33} & 0 & 0 & 0 & 0 \\
0 & 0 & 0 & d_{44} & 0 & 0 & 0 \\
0 & 0 & 0 & 0 & d_{55} & 0 & 0 \\
0 & 0 & 0 & 0 & 0 & d_{66} & 0 \\
0 & 0 & 0 & 0 & 0 & 0 & d_{77}
\end{bmatrix} \dot{\dot{v}}_{z} \tag{12}$$

Coriolis and Centripetal vector:

$$\underline{C}[\underline{\dot{q}},\underline{q}] = \begin{bmatrix}
c_{11} & c_{12} & c_{13} & 0 & c_{15} & 0 & 0 \\
c_{21} & c_{22} & c_{23} & 0 & c_{25} & 0 & 0 \\
c_{31} & c_{32} & c_{33} & 0 & c_{35} & 0 & 0 \\
c_{41} & c_{42} & c_{43} & 0 & 0 & 0 & 0 \\
c_{51} & c_{52} & c_{53} & 0 & c_{55} & 0 & 0 \\
c_{61} & 0 & c_{63} & 0 & c_{65} & 0 & 0 \\
c_{71} & c_{72} & c_{73} & 0 & c_{75} & 0 & 0
\end{bmatrix} \begin{bmatrix} \dot{\phi}_D \\ \dot{\phi}_A \\ \dot{\phi}_S \\ \dot{l}_A \\ \dot{\alpha}_x \\ \dot{\nu}_y \\ \dot{\nu}_z \end{bmatrix} + \begin{bmatrix} 0 & z_{12} & z_{13} & 0 & z_{15} & 0 & 0 \\
z_{21} & 0 & z_{23} & 0 & z_{25} & 0 & 0 \\
z_{21} & 0 & z_{23} & 0 & z_{25} & 0 & 0 \\
z_{31} & z_{32} & 0 & 0 & z_{35} & 0 & 0 \\
z_{31} & z_{32} & 0 & 0 & z_{35} & 0 & 0 \\
z_{41} & z_{42} & z_{43} & 0 & 0 & 0 & 0 \\
z_{51} & z_{52} & z_{53} & 0 & 0 & 0 & 0 \\
z_{51} & z_{52} & z_{53} & 0 & 0 & 0 & 0 \\
z_{61} & 0 & z_{63} & 0 & z_{65} & 0 & 0 \\
z_{71} & z_{72} & z_{73} & 0 & z_{75} & 0 & 0
\end{bmatrix} \begin{bmatrix} \dot{\phi}_D^2 \\ \dot{\phi}_A^2 \\ \dot{\phi}_A^2 \\ \dot{\phi}_S^2 \\ \dot{z}_{41} \\ z_{51} & z_{52} & z_{53} & 0 & 0 & 0 & 0 \\
z_{61} & 0 & z_{63} & 0 & z_{65} & 0 & 0 \\
z_{71} & z_{72} & z_{73} & 0 & z_{75} & 0 & 0
\end{bmatrix} \begin{bmatrix} \dot{\phi}_D^2 \\ \dot{\phi}_A^2 \\ \dot{\phi}_A^2 \\ \dot{\phi}_S^2 \\ \dot{z}_{41}^2 \\ z_{51} & z_{52} & z_{53} & 0 & 0 & 0 & 0 \\
z_{61} & 0 & z_{63} & 0 & z_{65} & 0 & 0 \\
z_{71} & z_{72} & z_{73} & 0 & z_{75} & 0 & 0
\end{bmatrix} \begin{bmatrix} \dot{\phi}_D^2 \\ \dot{\phi}_A^2 \\ \dot{\phi}_A^2 \\ \dot{z}_{51} \\ \dot{z}_{61} & 0 & z_{63} & 0 & z_{65} & 0 & 0 \\
z_{71} & z_{72} & z_{73} & 0 & z_{75} & 0 & 0
\end{bmatrix} \begin{bmatrix} \dot{\phi}_D^2 \\ \dot{\phi}_A^2 \\ \dot{\phi}_A^2 \\ \dot{z}_{51} \\ \dot{z}_{61} & 0 & z_{63} & 0 & z_{65} & 0 & 0 \\
z_{71} & z_{72} & z_{73} & 0 & z_{75} & 0 & 0
\end{bmatrix} \begin{bmatrix} \dot{\phi}_D^2 \\ \dot{\phi}_A^2 \\ \dot{\phi}_A^2 \\ \dot{\phi}_A^2 \\ \dot{z}_{51} \\ \dot{z}_{61} & 0 & z_{63} & 0 & z_{65} & 0 & 0 \\
z_{71} & z_{72} & z_{73} & 0 & z_{75} & 0 & 0
\end{bmatrix} \begin{bmatrix} \dot{\phi}_D^2 \\ \dot{\phi}_A^2 \\ \dot{\phi}_A^2 \\ \dot{\phi}_A^2 \\ \dot{z}_{51} \\ \dot{z}_{61} & 0 & z_{63} & 0 & z_{65} & 0 & 0 \\
z_{71} & z_{72} & z_{73} & 0 & z_{75} & 0 & 0
\end{bmatrix} \begin{bmatrix} \dot{\phi}_D^2 \\ \dot{\phi}_A^2 \\ \dot{\phi}_A^$$

Stiffness matrix:

$$\underline{K}\underline{q} = \begin{bmatrix}
0 & 0 & 0 & 0 & 0 & 0 & 0 & 0 \\
0 & 0 & 0 & 0 & 0 & 0 & 0 & 0 \\
0 & 0 & 0 & 0 & 0 & 0 & 0 & 0 \\
0 & 0 & 0 & 0 & 0 & 0 & 0 & 0 \\
0 & 0 & 0 & 0 & k_{55} \stackrel{?}{=} c_{\alpha x} & 0 & 0 & 0 \\
0 & 0 & 0 & 0 & 0 & k_{66} \stackrel{?}{=} c_{\nu y} & 0 & v_{y} \\
0 & 0 & 0 & 0 & 0 & 0 & k_{77} \stackrel{?}{=} c_{\nu z}
\end{bmatrix} \begin{bmatrix} \varphi_{D} \\ \varphi_{A} \\ \varphi_{S} \\ l_{A} \\ \alpha_{x} \\ v_{y} \\ v_{z} \end{bmatrix} \tag{14}$$

15

5

10

(The elements of the stiffness matrix depend heavily on the run-out length of the ladder. A function which reflects this dependence is calculated from simulations.)

Gravitation vector:

(15)

20

30

35

40

45

etc.

[0036] In the following, the equations of motion of subsystems, necessary for the setting up of the state-space model and the computation of the following control unit, are specified. The elements of the equations of motion listed in the following are in part quite extensive so that a detailed description will be dispensed with here. It is only mentioned here that the elements of the following equations of motion are generally non-linearly dependent on various system variables such as, for example, the equivalent masses, moments of inertia, the various angles of the rotational degree of freedom

 $\underline{G}[\underline{q}] = \begin{vmatrix} g_{21} \\ g_{31} \\ g_{41} \\ 0 \\ 0 \end{vmatrix}$

[0037] Subsystem rotation:

• Equation of motion for φ_D :

$$m_{11}\ddot{\varphi}_D + m_{15}\ddot{\alpha}_x + m_{16}\ddot{v}_y + c_{11}\dot{\varphi}_D + c_{13}\dot{\alpha}_x + d_{11}\dot{\varphi}_D = M_D$$
 (16)

• Equation of motion for α_x :

$$m_{5I}\ddot{\varphi}_D + m_{55}\ddot{\alpha}_x + m_{56}\ddot{v}_v + k_{55}\alpha_x + c_{5I}\dot{\varphi}_D + c_{53}\dot{\varphi}_S + d_{55}\dot{\alpha}_x = 0$$
 (17)

55

• Equation of motion for v_Y :

$$m_{61}\ddot{\varphi}_D + m_{65}\ddot{\alpha}_x + m_{66}\ddot{v}_v + k_{66}v_v + c_{61}\dot{\varphi}_D + c_{63}\dot{\varphi}_S + d_{66}\dot{v}_v = 0$$
(18)

[0038] Subsystem elevation/inclination:

• Equation of motion for φ_A :

5

10

15

25

30

45

55

$$m_{22}\ddot{\varphi}_{A} + m_{23}\ddot{\varphi}_{S} + m_{24}\ddot{l}_{A} + m_{27}\ddot{v}_{z} + g_{21} + c_{21}\dot{\varphi}_{D} + c_{22}\dot{\varphi}_{A} + z_{21}\dot{\varphi}_{D}^{2} + z_{23}\dot{\varphi}_{S}^{2} + z_{25}\dot{\alpha}_{x}^{2} + d_{22}\dot{\varphi}_{A} = M_{A}$$
(19)

• Equation of motion for φ_K :

$$m_{32}\ddot{\varphi}_{A} + m_{33}\ddot{\varphi}_{S} + m_{34}\ddot{l}_{A} + m_{37}\ddot{v}_{z} + g_{31} + c_{31}\dot{\varphi}_{D} + c_{32}\dot{\varphi}_{A} + z_{31}\dot{\varphi}_{D}^{2} + z_{32}\dot{\varphi}_{A}^{2} + z_{35}\dot{\alpha}_{x}^{2} + d_{33}\dot{\varphi}_{S} = M_{K}$$

$$(20)$$

• Equation of motion for I_A :

$$m_{42}\ddot{\varphi}_{A} + m_{43}\ddot{\varphi}_{S} + m_{44}\ddot{l}_{A} + g_{41} + c_{41}\dot{\varphi}_{D} + c_{42}\dot{\varphi}_{A} + z_{41}\dot{\varphi}_{D}^{2} + z_{42}\dot{\varphi}_{A}^{2} + z_{43}\dot{\varphi}_{S}^{2} + d_{44}\dot{l}_{A} = M_{IA}$$

$$(21)$$

• Equation of motion for v_z :

$$m_{72}\ddot{\varphi}_{A} + m_{73}\ddot{\varphi}_{S} + m_{77}\ddot{v}_{z} + g_{71} + c_{71}\dot{\varphi}_{D} + c_{72}\dot{\varphi}_{A} + z_{71}\dot{\varphi}_{D}^{2} + z_{72}\dot{\varphi}_{A}^{2} + z_{73}\dot{\varphi}_{S}^{2} + z_{75}\dot{\alpha}_{x}^{2} + d_{77}\dot{v}_{z} + k_{77}v_{z} = 0$$
(22)

[0039] In the following, the state-space model for the subsystem rotation will firstly be derived which then forms the basis for the design of the controller and pilot control.

[0040] The drive torque M_D , from Equ. 16, supplied by a corresponding hydraulic motor, can be described by the following equations:

$$M_{D} = i_{D} \frac{V_{D}}{2\pi} \Delta p_{D}$$

$$\Delta \dot{p}_{D} = \frac{1}{V_{D} \beta} (Q_{FD} - i_{D} \frac{V_{D}}{2\pi} \dot{\phi}_{D})$$

$$Q_{FD} = K_{PD} u_{StD}$$
(23)

Whereby

 M_D denotes drive torque

5

10

15

20

25

30

35

40

45

 Δp_D denotes pressure difference

 $\dot{\phi}_D$ denotes angular velocity

Q_{FD} denotes hydraulic oil flow rate

 u_{StD} denotes control voltage servo valve without backlash

 i_D denotes transmission ratio

 V_D denotes displacement volume of hydraulic motor

β denotes hydraulic oil compressibility

 K_{PD} denotes proportionality factor

[0041] The equations 10 to 23 can also be used to estimate the bending signals from the pressure signals of the hydraulic drives by designing an observer.

[0042] For the state-space representation of the system and the subsequent controller computation, the following simplification can be applied for the hydraulic drive units, taking into account the auxiliary flow rate control:

$$Q_{FD} = \frac{K_{PD}}{1 + sT} u_{StD} \tag{24}$$

[0043] T is a time delay constant which is determined from measurements on real systems. By assuming $\Delta \dot{p}_D = 0$ (steady state) the following relationship is obtained:

$$0 = \frac{1}{V_D \beta} (Q_{FD} - i_D \frac{V_D}{2\pi} \dot{\varphi}_D) \xrightarrow{Umstellen} Q_{FD} = i_D \frac{V_D}{2\pi} \dot{\varphi}_D$$
 (25)

[0044] If equations 24 and 25 are equated and the resulting expression is correspondingly rearranged with respect to $\ddot{\phi}_D$, the following expression results:

$$\ddot{\varphi}_D = \frac{K_{PD} 2\pi}{i_D V_D T} \cdot u_{SlD} - \frac{1}{T} \cdot \dot{\varphi}_D \tag{26}$$

[0045] A further simplification consists of neglecting the Coriolis and centripetal terms in the equations 16 to 18 on account of their small effect. By applying the simplifications described, the representation of the equations of motion for the subsystem rotation in state-space form is as follows:

$$\dot{\underline{x}}_{D} = \underline{A}_{D}\underline{x}_{D} + \underline{B}_{D}\underline{u}_{D}
\underline{y}_{D} = \underline{C}_{D}\underline{x}_{D}$$
(27)

55 with:

State vector
$$\underline{x}_{D} = \begin{bmatrix} \dot{\varphi}_{D} \\ \alpha_{x} \\ \dot{\alpha}_{x} \\ v_{y} \\ \dot{v}_{y} \end{bmatrix}$$
 (28)

Control value:
$$u_D = u_{StD}$$
 (29)

Output value:
$$y_D = \dot{\varphi}_D$$
 (30)

[0046] With the form of state vector chosen in Equ. 28, one firstly obtains the relationship

$$\begin{bmatrix}
1 & 0 & 0 & 0 & 0 \\
m_{51} & 0 & m_{55} & 0 & m_{56} \\
0 & 1 & 0 & 0 & 0 \\
m_{61} & 0 & m_{65} & 0 & m_{66} \\
0 & 0 & 0 & 1 & 0
\end{bmatrix} \cdot \underline{\dot{x}_{D}} = \begin{bmatrix}
-\frac{1}{T} & 0 & 0 & 0 & 0 \\
0 & -k_{55} & -d_{55} & 0 & 0 \\
0 & 0 & 1 & 0 & 0 \\
0 & 0 & 0 & -k_{66} & -d_{66} \\
0 & 0 & 0 & 0 & 1
\end{bmatrix} \cdot \underline{x_{D}} + \begin{bmatrix}
\frac{K_{PD} 2\pi}{i_{D} V_{D} T} \\
0 \\
0 \\
0
\end{bmatrix} \cdot \underline{u_{D}}$$
(31)

[0047] The system and input matrices A_D and B_D result from multiplication of the matrix equation 31 with the inverse of H. The composition is only shown schematically here, on account of the complexity of the individual elements:

$$\underline{A_D} = \begin{bmatrix} a_{11} & 0 & 0 & 0 & 0 \\ 0 & 0 & 1 & 0 & 0 \\ a_{31} & a_{32} & a_{33} & a_{34} & a_{35} \\ 0 & 0 & 0 & 0 & 1 \\ a_{51} & a_{52} & a_{53} & a_{54} & a_{55} \end{bmatrix} \qquad \underline{B_D} = \begin{bmatrix} b_1 \\ 0 \\ b_3 \\ 0 \\ b_5 \end{bmatrix}$$
(32)

[0048] From Equ. 30 the output vector \underline{C}_D produces:

$$C_D = \begin{bmatrix} 1 & 0 & 0 & 0 & 0 \end{bmatrix} \tag{33}$$

[0049] The dynamic model of the axis of rotation is interpreted as a changeable parameter system with respect to run-out length I, angle of elevation φ_A and articulation angle φ_K . The derived state equations are the basis for the pilot control 71 and state controller 73 described in the following design (Fig. 7). Input variables of the pilot control block 71

are the reference angular velocity $\dot{\phi}_{Dref}$ the reference angular acceleration $\ddot{\phi}_{Dref}$ and the reference jerking $\dddot{\phi}_{Dref}$ (if necessary also the derivative of the reference jerking). The command variable \underline{w}_D is thus

$$\underline{w}_{D} = \begin{bmatrix} \dot{\varphi}_{Dref} \\ \ddot{\varphi}_{Dref} \\ \ddot{\varphi}_{Dref} \end{bmatrix} \tag{34}$$

[0050] The components of \underline{w}_D are weighted with the pilot control gains K_{VD0} to K_{VD2} and the total fed to the servo input. The pilot control block 71 is supported by a state controller 73, as the dynamic model, as already mentioned, only abstractly reproduces the real relationships and can also react to non-deterministic disturbance (e.g. wind effects, load fluctuations in the cage, etc.) with the aid of the controller. At least one of the quantities to be measured of the state vector (Equ. 28) is weighted with a control gain and fed back to the servo input. There the difference between the output value of the pilot control block 71 and the output value of the state controller block 73 is generated. The following goes into the computation of the pilot control gains in more detail. If the state controller is available, as is always assumed in the following, this must be taken into account in the computation of the pilot control gains. (Without state controller the feedback in Equ. 34 would no longer apply and only the system matrix A_D taken into account in the relationship above. The procedure then continues in the same way.)

[0051] The state-space representation from Equ. 27 is expanded, taking into account pilot control and controller feedback, to:

$$\frac{\dot{x}_D = (\underline{A}_D - \underline{B}_D \underline{K}_D)\underline{x}_D + \underline{B}_D \underline{S}_D \underline{w}_D}{y_D = \underline{C}_D \underline{x}_D}$$
(35)

with the pilot control matrix:

5

10

15

20

25

30

35

40

45

50

55

$$S_{D} = \begin{bmatrix} K_{VD0} & K_{VD1} & K_{VD2} \end{bmatrix}$$
 (36)

and the pilot control gains K_{VD0} to K_{VD2} (to be calculated). After analysis of Equ. 35, the output voltage of the pilot control block is given by:

$$u_{DVorst} = K_{VD0}\dot{\phi}_{Dref} + K_{VD1}\ddot{\phi}_{Dref} + K_{VD2}\ddot{\phi}_{Dref} \tag{37}$$

[0052] The individual pilot control coefficients are calculated as follows. The Laplace transformation of Equ. 35 leads

to the following result:

20

45

50

55

$$\underline{x}_{D} = (s\underline{I} - \underline{A}_{D} + \underline{B}_{D}\underline{K}_{D})^{-1} \cdot \underline{B}_{D}\underline{S}_{D} \begin{bmatrix} w_{D} \\ sw_{D} \\ s^{2}w_{D} \end{bmatrix} = (s\underline{I} - \underline{A}_{D} + \underline{B}_{D}\underline{K}_{D})^{-1} \cdot \underline{B}_{D}\underline{S}_{D} \begin{bmatrix} 1 \\ s \\ s^{2} \end{bmatrix} \cdot w_{D}(s)$$

$$\underline{y}_{D}(s) = \underline{C}_{D} \cdot (s\underline{I} - \underline{A}_{D} + \underline{B}_{D}\underline{K}_{D})^{-1} \cdot \underline{B}_{D}\underline{S}_{D} \begin{bmatrix} 1 \\ s \\ s^{2} \end{bmatrix} \cdot w_{D}(s)$$

$$(38)$$

[0053] From this results the control transfer function given below (the output value $y_D(s)$ corresponds to the rotational velocity from Equ. 30):

$$\frac{y_D(s)}{w_D(s)} = \underbrace{\frac{b_0 + b_1 s \dots + b_{n-2} s^{n-2}}{N(s)} \left(K_{VD0} + K_{VD1} s + K_{VD2} s^2 \right)}_{\widetilde{G}_D(s)}$$
(39)

[0054] The output value thus follows the command variable exactly if $\tilde{G}_D(s) \approx 1$ is valid. In this case one obtains an ideal system performance with respect to the rotational velocity, the acceleration and the jerking. Although these requirements cannot be met fully, a favourable performance can be achieved, if the following conditions are fulfilled:

$$\widetilde{G}_{D}(s) = 1 = \frac{\widetilde{b}_{0}(K_{VDi}) + \widetilde{b}_{1}(K_{VDi})s + \widetilde{b}_{2}(K_{VDi})s^{2} + \dots}{a_{0} + a_{1}s + a_{2}s^{2} + \dots}$$

$$a_{0} = \widetilde{b}_{0}(K_{VDi})$$

$$a_{1} = \widetilde{b}_{1}(K_{VDi})$$

$$a_{2} = \widetilde{b}_{2}(K_{VDi})$$

$$\vdots$$

$$(40)$$

[0055] The set of linear equations above can be solved analytically for the unknown pilot control gains K_{VD0} to K_{VD2} . The representation of the transfer function $\widetilde{G}_D(s)$ from Equ. 39 is dispensed with here, owing to the complexity of the entire system.

[0056] The pilot control gains are available henceforth dependent on the elements of the mass matrix, the damping matrix, the stiffness matrix and further model parameters. The corresponding matrix elements are in turn dependent on further characteristics, such as the angle of elevation, the articulation angle, the run-out length etc. If these parameters change, then the pilot control gains also change automatically, so that the vibration damping behaviour of the pilot control is maintained while moving the cage. Moreover, a dependency of the pilot control coefficients upon the control gains k_{1D} to k_{5D} can be identified in the pilot control gains. Their derivation is explained in the following section of the description of the invention.

[0057] The control feedback 73 is configured as state controller. A state controller is characterised in that every state parameter, that is every component of the state vector \underline{x}_D is weighted with a control gain k_{iD} and is fed back to the servo

input of the control system.

15

20

25

40

45

[0058] The control gains k_{iD} are combined as the feedback vector K_D .

[0059] According to "Unbehauen, Regelungstechnik 2, a. a. O.", the dynamic behaviour of the system is determined by the position of the eigen- values of the system matrix \underline{A}_D , which, at the same time, are poles of the transfer function in the frequency range. The eigen-values of the matrix can be determined as follows by calculating the zeros from the determinants with respect to the variables s of the characteristic polynomials.

$$\det(s\underline{I} - \underline{A}_D) \equiv 0 \tag{42}$$

[0060] *I* is the unit matrix. In the case of the chosen state-space model from Equ. 32, the analysis of Equ. 42 leads to a fifth order polynomial with the general form:

$$s^5 + a_4 s^4 + a_3 s^3 + a_2 s^2 + a_1 s + a_0 \equiv 0$$
 (43)

[0061] These eigen-values can be selectively displaced by feeding back the state variables via the control matrix \underline{K}_D to the control input, as the position of the eigen-values is now determined by the analysis of the following determinants:

$$\det(sI - \underline{A}_D + \underline{B}_D \cdot \underline{K}_D) \equiv 0 \tag{44}$$

[0062] The analysis of Equ. 44 leads again to a fifth order polynomial which is now, however, dependent on the control gains k_{iD} (i=1..5). In the case of the model from Equ. 32, Equ. 43 becomes

$$s^{5} + a_{4}(k_{5D}, k_{3D}, k_{1D})s^{4} + a_{3}(k_{5D}, k_{4D}, k_{3D}, k_{2D}, k_{1D})s^{3} + a_{2}(k_{5D}, k_{4D}, k_{3D}, k_{2D}, k_{1D})s^{2} + a_{1}(k_{4D}, k_{1D}, k_{1D})s + a_{0}(k_{1D}) \equiv 0$$

$$(45)$$

[0063] It is now required that the Equ. 44 and 45 respectively adopt particular zeros through the control gains k_{iD} in order to selectively influence the system dynamics which is reflected in the zeros of this polynomial. The way the poles are located is known from the calculation of the open-loop poles for the subsystem rotation (Equ. 42). There exists a negative real pole (conditional on the time delay constant of the hydraulics from Equ. 24) and one each of conjugated complex pole pairs conditional upon the bending and torsion. With this a priori knowledge, the following structure of the pole specifying polynomial results:

$$p_{D}(s) = (s - p_{h}) \cdot (s - (p_{\alpha,r} + i \cdot p_{\alpha,im})) \cdot (s - (p_{\alpha,r} - i \cdot p_{\alpha,im})) \cdot (s - (p_{\nu_{y,r}} + i \cdot p_{\nu_{y,im}})) \cdot (s - (p_{\nu_{y,r}} - i \cdot p_{\nu_{y,im}}))$$
(46)

p_h Hydraulic pole

 $p_{\alpha,r}$ Real part torsion pole

 $p_{lpha,im}$ Imaginary part torsion pole

 $p_{v_y,r}$ Real part bending pole

 $p_{v_{\!\scriptscriptstyle V\!\!,im}}$ Imaginary part bending pole

[0064] In this connection, the conjugated complex poles are not addressed individually but through direct access to the real and imaginary parts. In this way one can selectively influence the vibration and damping for torsion and bending of the arm by the adjustment of the controller. The control coefficients are therefore a function of the real and imaginary parts of the pole.

[0065] The pole positions are to be chosen from Equ. 46 in such a way that the system is stable, the controller works adequately fast with good damping and the limit of the variables is not reached under the typically arising control deviations. The exact values can be established before initial operation via simulation according to these criteria.

[0066] The control gains can now be determined by comparing coefficients of the polynomials Equ. 46 and 44.

15

20

5

$$\det(sI - A_D + \underline{B}_D \cdot \underline{K}_D) \equiv p_D(s) \tag{47}$$

[0067] Based on Equ. 47, there results a set of linear equations to be solved dependent on the control gains k_{iD} . The analysis of this set of equations leads to analytic expressions for the respective control gains dependent upon the desired poles from Equ. 46 and the individual system parameters. If these parameters change, as for example the angle of articulation or the run-out length, then these changes are immediately taken into account by a variation of the individual control parameters. A separate description of the individual control coefficients will be dispensed with here on account of the complexity of the individual expressions.

[0068] With feedback of $\dot{\phi}_D$, α_x , $\dot{\alpha}_x$, v_v , \dot{v}_v , the output of the state controller block 73 is then

$$u_{Drick} = k_{1D}\dot{\phi}_D + k_{2D}\alpha_x + k_{3D}\dot{\alpha}_x + k_{4D}\nu_y + k_{5D}\dot{\nu}_y \tag{48}$$

[0069] Taking into account the pilot control 71, the reference control voltage of the proportional valve for the axis of rotation is then

35

30

$$u_{Dref} = u_{Dvorst} - u_{Drück} \tag{49}$$

40

45

50

[0070] The states $\dot{\phi}_D$, α_x , $\dot{\alpha}_x$, v_y , \dot{v}_y of the subsystem rotation being considered are either directly or indirectly measured by suitable sensors. The angular velocity is generally measured with corresponding encoders on the swivel joint. If strain gauges (SG) are used as measurement pick-up sensors for the elastic degrees of freedom, it follows to locate these in corresponding positions on the ladder unit. For example, two SGs can be installed right- and left-sided respectively on the lower and upper rails of the ladder in a vertical preferred direction (vertical SG) and horizontal preferred direction (horizontal SG), so that a differential sensitivity results with torsional deflections. Thus horizontal bending motions as well as torsional motions are measured coupled by means of this installation of the SGs. The signals are decoupled according to the invention by means of a measurement data signal conditioner 75, so that the feedback law (48) can be achieved. It is thereby assumed that the difference signal of the vertical SG is a suitable measure of the torsional angle.

[0071] Static tests for the torsion and bending can be drawn upon to calibrate the SG signals. From this results

$$\alpha_{x} = k_{t} \frac{(\varepsilon_{vr} - \varepsilon_{vl}) \cdot l_{A}^{3}}{(l_{A} - l_{0v})}$$
(49a)

with

5

10

15

ε_ν - Strain at SG position (vertical SG)

 I_{0v} - SG position (distance from the fixing point in the x direction)

k_t - proportionality factor

[0072] The horizontal bending essentially has an effect on the difference signal of the horizontal SG. As mentioned, it is also influenced by the torsion of the ladder. Assuming

$$\varepsilon_{hr} - \varepsilon_{hl} = \frac{l_A - l_{0h}}{l_A^3} \cdot \frac{v_y}{k_h} + \frac{l_A - l_{0h}}{l_A^3} \cdot \frac{\alpha_x}{k_{th}}$$
(49b)

one obtains

$$v_{y} = k_{h} \frac{\left(\varepsilon_{hr} - \varepsilon_{hl}\right) \cdot l_{A}^{3}}{l_{A} - l_{0h}} - \frac{k_{h} \alpha_{x}}{k_{th}} \tag{49c}$$

25 with

30

35

40

50

 ε_h - Strain at SG position (horizontal SG)

 I_{0h} - SG position (distance from the fixing point in the x direction)

k_h - proportionality factor

k_{th} - proportionality factor

[0073] This can be summarised as the solution to a set of linear equations

$$\begin{bmatrix} v_{y} \\ \alpha_{x} \end{bmatrix} = \begin{bmatrix} \frac{l_{A} - l_{0h}}{l_{A}^{3} k_{h}} & \frac{l_{A} - l_{0h}}{l_{A}^{3} k_{th}} \\ 0 & \frac{l_{A} - l_{0v}}{l_{A}^{3} k_{t}} \end{bmatrix}^{-1} \begin{bmatrix} \varepsilon_{hr} - \varepsilon_{hl} \\ \varepsilon_{vr} - \varepsilon_{vl} \end{bmatrix}$$

$$(49d)$$

45 **[0074]** The corresponding time derivatives of the decoupled bending states can be implemented with the aid of suitable real differentiator modules.

[0075] In the context of the calculation for active vibration damping, the articulated ladder is considered as a discrete multiple body system with three point masses and corresponding spring and damper elements. In practice, dynamic effects occur which are not thereby taken into account. As there exists a system with locally distributed parameters, higher harmonics occur, for example, which are correspondingly recorded by the sensor elements and thereby coupled in the signal flow of the control feedback. The control behaviour is thus negatively influenced. On the other hand, it can happen that the measurement signal of the elastic degrees of freedom has an offset. This can lead to a non-damped rotary motion. In order to solve this problem, the processing of measured data can be supplemented by a disturbance observer with the following functions:

55

- 1.) Correction of offsets on the measured signal inherent in the measuring principle.
- 2.) Elimination of frequency content on the measuring signal, caused by ladder higher harmonics.

[0076] As a result, for the signal processing, one disturbance observer is used for the torsional vibrations and the horizontal bending vibrations respectively. The vibration differential equation which describes the progression of the vibrations to be actively damped is represented as follows:

$$\ddot{\varphi}_{\alpha x, \nu y} = -w_{\alpha x, \nu y}^{2} \cdot \varphi_{\alpha x, \nu y} - 2d_{\alpha x, \nu y} w_{\alpha x, \nu y} \cdot \dot{\varphi}_{\alpha x, \nu y}$$
(49e)

[0077] The angular amplitude of the vibration $\varphi_{\alpha x, \nu y}$ is approximated by a 2^{nd} order damped differential equation with the parameters resonance frequency $\overline{\omega}_{\alpha x, \nu y}$ and damping $\overline{d}_{\alpha x, \nu y}$. It is essential here that the parameters are variable with respect to the system states, such as ladder length, angles of elevation and articulation or load masses. They can, for example, be obtained experimentally or from suitable physical models.

[0078] The angular offset error $\dot{\phi}_{offset,\alpha x,\nu y}$ is assumed to be constant in part.

$$\ddot{\varphi}_{offset,\alpha x,vy} = 0 \tag{49f}$$

[0079] In order to eliminate the ladder higher harmonics from the measurement signal, the resonance frequency $\overline{\omega}_{ober,\alpha x,\nu y}$ and the damping $\overline{d}_{ober,\alpha x,\nu y}$ are determined experimentally, these being also here generally dependent on the variable system parameters such as ladder length, angles of elevation and articulation and load masses. Alternatively, the resonance frequency and the damping can be determined from a suitable physical model description. The corresponding vibration differential equation of the harmonic is:

$$\ddot{\varphi}_{ober,\alpha x,vy} = -w_{ober,\alpha x,vy}^{2} \cdot \varphi_{ober,\alpha x,vy} - 2d_{ober,\alpha x,vy} w_{ober,\alpha x,vy} \cdot \dot{\varphi}_{ober,\alpha x,vy}$$
(49g)

[0080] The state-space representation from the previous sub-models shows:

$$\frac{\dot{x}_{\alpha x, vy}}{y_{m \alpha x, vy}} = \underline{A}_{\alpha x, vy} \cdot \underline{x}_{\alpha x, vy} + \underline{B}_{\alpha x, vy} \cdot \underline{u}_{\alpha x, vy}
y_{m \alpha x, vy} = \underline{C}_{\alpha x, vy} \cdot \underline{x}_{\alpha x, vy}$$
(49h)

whereby the following matrices and vectors are adopted:

State vector:
$$\underline{x}_{\alpha x, vy} = \begin{bmatrix} \varphi_{\alpha x, vy} \\ \dot{\varphi}_{\alpha x, vy} \\ \varphi_{Offset}_{\alpha x, vy} \\ \varphi_{Ober \alpha x, vy} \\ \dot{\varphi}_{Ober \alpha x, vy} \end{bmatrix}$$
Input matrix:
$$\underline{B}_{\alpha x, vy} = \begin{bmatrix} 0 \\ 1 \\ 0 \\ 0 \\ 0 \end{bmatrix}$$

55

5

10

15

20

35

40

System matrix:

5

10

15

20

25

30

35

40

45

50

55

Output matrix: $\underline{C}_{\alpha x, \nu y} = \begin{bmatrix} 1 & 0 & 1 & 1 & 0 \end{bmatrix}$ (49i)

[0081] According to the invention, the disturbance signal portions are eliminated from the measurement signal with an estimation procedure supported by an observer. A complete observer is derived in the case at hand. The observer equation for the modified state-space model is thus:

 $\hat{\underline{x}}_{\alpha x, vy} = (\underline{A}_{\alpha x, vy} - \underline{H}_{\alpha x, vy} \underline{C}_{\alpha x, vy}) \cdot \underline{x}_{\alpha x, vy} + \underline{B}_{\alpha x, vy} \cdot \underline{u}_{\alpha x, vy} + \underline{H}_{\alpha x, vy} \underline{y}_{m_{\alpha x, vy}}$ (49j)

[0082] The disturbance observer matrix $\underline{H}_{\alpha x, vy} = [h_{\alpha x, vy, 1}, h_{\alpha x, vy, 2}, h_{\alpha x, vy, 3}, h_{\alpha x, vy, 4}, h_{\alpha x, vy, 5}]^T$ is calculated, for example, according to the Riccati design procedure. It is essential here that the variable parameters such as ladder length, angle of elevation and load masses are likewise taken into account in the observer by adapting the observer differential

equation and the observer gains. The estimated values for $\dot{\phi}_{\alpha x, vy}$ and $\hat{\phi}_{\alpha x, vy}$ from the disturbance observer can be fed directly to the state controller. In this way the function of vibration damping can be improved significantly.

[0083] As an alternative to the observer-based elimination of higher harmonics, the feedback gain of the state controller 73 during the rotational motion can also be attenuated by means of the proportional attenuator 72. In this way, the control function for the ladder at standstill can be improved if no observer-based elimination has been performed.

[0084] The individual components of the axis controller for the axis of rotation are thereby explained. As a result, the combination of position path planning module and rotation axis controller fulfils the requirement for a vibration-free and position path-accurate movement with the axis of rotation.

[0085] In the following, the axis controller for the axis of elevation/ inclination 7 will be explained by using the results from the derivation of the control module for the axis of rotation. Fig. 8 shows the basic structure of the axis controller for the axis of elevation/inclination.

[0086] The output functions of the position path planning module, in the form of the reference cage velocity in the direction of the axis of elevation/inclination as well as its derivatives (acceleration, jerking and, if necessary, derivative of the jerking) are given to the pilot control block 91 (corresponds to block 71 for the axis of rotation). These functions are amplified in the pilot control block in such a way that there results a position path-accurate steering of the ladder without vibrations under the idealised conditions of the dynamic model. The basis for the determination of the pilot control gains is the dynamic model which will be derived in the following sections for the axis of elevation/inclination. In this way, under idealised conditions, the vibration of the ladder is suppressed and the cage follows the generated position path. **[0087]** As with the axis of rotation, the pilot control can optionally be supplemented by a state controller block 93 to compensate for disturbances (e.g. wind effects) and modelling errors (cf. axis of rotation 73). In this block at least one of the quantities to be measured, angle of elevation φ_{K_1} run-out length 1, bending of the ladder

in the vertical direction v_z or the derivative of the vertical bending \dot{v}_z , is amplified and fed back to the servo input. The derivative of the measurements φ_A and \dot{v}_z is formed numerically in the microprocessor control.

[0088] The value for the servo input formed from the pilot control u_{Avorst} and the optional state controller output $u_{Ar\ddot{u}ck}$ is then fed to the proportional valve for the cylinder of the axis of elevation/inclination of the hydraulic circuit.

[0089] The derivation of the dynamic model for the elevation axis which is the basis for the calculation of the pilot control gains and the state controller will now be exemplified.

[0090] The kinematics of the elevation/inclination axis is shown in Fig. 9. The actuation occurs by means of two hydraulic cylinders, whereby the position and speed of the ram are to be taken into account in the model. The actuation moment M_A from Equ. 19 can be described by the following equations:

(50)

 $M_{A} = F_{ZylA} d_{bA} \cos \varphi_{PA}$ $F_{ZylA} = p_{ZylA} A_{ZylA}$ $\dot{p}_{ZylA} = \frac{2}{\beta V_{ZylA}} \left(Q_{FA} - A_{ZylA} \dot{z}_{ZylA} \right)$ $Q_{FA} = K_{PA} \overline{u}_{StA}$ $z_{ZylA} = \sqrt{d_{aA}^2 + d_{bA}^2 - 2d_{aA}} d_{bA} \cos(\varphi_A + \varphi_{0A})$ $\dot{z}_{ZylA} = \frac{d_{aA} d_{bA} \sin(\varphi_A + \varphi_{0A})}{z_{ZylA}} \dot{\varphi}_{A}$

 $\cos \varphi_{PA} = \frac{d_{aA} \sin(\varphi_A + \varphi_{0A})}{z_{zylA}}$

whereby

30

35

45

50

5

10

 M_A denotes actuation moment ϕ_{PA} denotes projection angle

 $\begin{array}{ll} P_{Zy|A} & \text{denotes pressure in hydraulic cylinder} \\ A_{Zy|A} & \text{denotes effective cross-sectional area} \\ \dot{\phi}_A & \text{denotes angular velocity elevation/inclination} \end{array}$

 $\begin{array}{ll} Z_{ZyIA} & \text{denotes position of the ram} \\ Q_{FA} & \text{denotes volume flow of hydraulic oil} \\ u_{StA} & \text{denotes activation voltage of servo valve} \end{array}$

 $u_{\mathit{StA.min}}$ denotes minimum activation voltage of servo valve

 $\overline{u}_{\mathit{StA}}$ denotes working activation voltage

 V_{ZyIA} denotes volume of hydraulic cylinder (each cylinder)

β denotes compressibility of hydraulic oil

 K_{PA} denotes proportionality factor

 d_{aA} denotes distance pivot point to attachment point of hydraulic cylinder on ladder gear unit denotes distance pivot point to attachment point of hydraulic cylinder on ladder unit

 φ_{OA} denotes angle, see Fig. 9

[0091] The bending and torsion signals can also be estimated for the elevation axis from the pressure signals of Equ. 50 via an observer, as for the axis of rotation.

[0092] By neglecting the Coriolis and centripetal terms, as well as the angular acceleration of the articulated arm $\ddot{\phi}_{\mathcal{K}}$, Equ. 22 serves as starting point for the compilation of the state-space model and consequently is presented as follows.

55

$$m_{77}\ddot{\varphi}_A + m_{77}\ddot{v}_z + g_{71} + d_{77}\dot{v}_z + k_{77}v_z = 0 \tag{51}$$

[**00** tak

5

10

[0093] The relationship shown in Equ. 50, for the calculation of pressure changes in the hydraulic cylinder \dot{p}_{ZyIA} , is taken as the basis for the following calculations. A first-order lag element is chosen as computational model for the determination by approximation of the variable Q_{FA} contained in the equation. Consequently, the dynamic aspects of a auxiliary flow rate control are taken into account in a simple approach. This simplification describes sufficiently accurately the correlation between the activation voltage and the volume flow of the hydraulic oil.

15

$$Q_{FA} = \frac{K_{PA}}{1 + sT} u_{StA} \tag{52}$$

20

[0094] Putting \dot{p}_{ZyIA} = 0 (steady state), the following relationship is obtained from Equ. 50:

25

$$0 = \frac{2}{V_{ZylA}\beta} (Q_{FA} - A_{ZylA} \dot{z}_{ZylA}) \xrightarrow{Umstellen} Q_{FA} = A_{ZylA} \cdot \dot{z}_{ZylA}$$
 (53)

30

[0095] By using the relationship between ram speed and speed of elevation from Equ. 50, the dependence of the volume flow on the speed of elevation results:

35

40

$$\dot{z}_{ZylA} = \underbrace{\frac{d_{aA}d_{bA}\sin(\varphi_A + \varphi_{0A})}{z_{Zyl,A}}}_{\Psi(q_A)} \cdot \dot{\varphi}_A \xrightarrow{Einsetzen} Q_{FA} = A_{ZylA} \cdot \Psi(\varphi_A) \cdot \dot{\varphi}_A$$
 (54)

45

[0096] Equating Equ. 52 (in the time domain) and 54 and subsequently rearranging the resulting expression for $\ddot{\phi}_A$, leads, after corresponding collecting of the coefficients, to the following expression.

50

$$\ddot{\varphi}_{A} = \frac{K_{PA}}{A_{ZylA} \cdot T \cdot \Psi} \cdot u_{SlA} + \left(-\frac{1}{T} - \frac{\dot{\Psi}}{\Psi}\right) \cdot \dot{\varphi}_{A}$$
 (55)

[0097] By using the derived relationship, the following representation of the equations of motion for the subsystem

55

elevation/inclination in state-space form is produced:

$$\frac{\dot{x}_{A}}{y} = \underline{A}_{A} \underline{x}_{A} + \underline{B}_{A} \underline{u}_{A}
\underline{y}_{A} = \underline{C}_{A} \underline{x}_{A}$$
(56)

with:

State vector:
$$\underline{x}_{A} = \begin{bmatrix} \dot{\varphi}_{A} \\ v_{z} \\ \dot{v}_{z} \end{bmatrix}$$
 (57)

$$u_A = u_{StA}$$

$$y_A = \Psi \dot{\varphi}_A$$

(61)

[0098] With the form of the state vector chosen in Equ. 57, one initially obtains the relationship

$$\begin{bmatrix} 1 & 0 & 0 \\ m_{72} & 0 & m_{77} \\ 0 & 1 & 0 \end{bmatrix} \cdot \dot{\underline{x}}_{A} = \begin{bmatrix} -\frac{1}{T} - \frac{\dot{\Psi}}{\Psi} & 0 & 0 \\ 0 & -k_{77} & -d_{77} \\ 0 & 0 & 1 \end{bmatrix} \cdot \underline{x}_{A} + \begin{bmatrix} \frac{K_{PA}}{A_{ZylA} \cdot T \cdot \Psi} \\ 0 \\ 0 \end{bmatrix} \cdot \underline{u}_{A}$$

[0099] The system and input matrices A_A and B_A are obtained by matrix multiplication of the inverses of \underline{H} in Equ. 60.

$$\underline{A}_{A} = \begin{bmatrix} -\frac{\Psi + \dot{\Psi}T}{\Psi T} & 0 & 0\\ 0 & 0 & 1\\ \frac{m_{72}(\Psi + \dot{\Psi}T)}{m_{77}\Psi T} & -\frac{k_{77}}{m_{77}} & -\frac{d_{77}}{m_{77}} \end{bmatrix} \qquad \underline{B}_{A} = \begin{bmatrix} \frac{K_{PA}}{A_{ZylA} \cdot T \cdot \Psi} \\ 0\\ -\frac{m_{72}K_{PA}}{m_{77}A_{ZylA}\Psi T} \end{bmatrix}$$

[0100] As the hydraulic cylinder ram speed is to be taken as output variable, the output vector \underline{C}_A , from Equ. 59, becomes:

$$\underline{C}_A = \begin{bmatrix} \Psi & 0 & 0 \end{bmatrix} \tag{62}$$

[0101] The dynamic model of the elevation/inclination axis is understood as a variable parameter system with respect to the run-out length I, the trigonometric function component of the angle of elevation φ_A and of the angle of articulation φ_K . The Equ. 56 - 62 form the basis for the design of the pilot control 91 and state controller 93, to be described now. **[0102]** Input variables of the pilot control block 91 are the reference angular velocity $\dot{\varphi}_{Aref}$ the reference angular

acceleration $\ddot{\varphi}_{Aref}$ and the reference jerking $\overset{\dots}{\varphi}_{Aref}$ (and, if necessary, the derivative of the reference jerking). The command variable vector w_A is thus

$$\underline{w}_{A} = \begin{bmatrix} \dot{\varphi}_{Aref} \\ \ddot{\varphi}_{Aref} \\ \ddot{\varphi}_{Aref} \end{bmatrix}$$
(63)

[0103] The components of \underline{w}_A are weighted with the pilot control gains K_{VA0} to K_{VA2} in the pilot control block 91 and their summation fed to the servo input. The pilot control block 91 is supported by a state controller 93, because as already mentioned, the dynamic model only reproduces the real relationships in an abstract way and, with the aid of the controller, non-deterministic disturbances (e.g. wind effects, load fluctuations in the cage, etc.) can also be reacted to. At least one of the measured quantities of the state vector from Equ. 57 is weighted with a control gain and fed back to the servo input. There, again, the difference between the output value of the pilot control block 91 and the output value of the state controller 93 is formed, analogue to the structure of the axis controller for the sub-system rotation. The existence of the state controller block, which should be assumed in the following, has to be taken account in the computation of the pilot control gains. (Without the state controller, the arrangement implemented in the derivation of the rotation axis controller is valid).

[0104] Taking into account the pilot control and the control feedback, the state controller from Equ. 56 expands to:

$$\frac{\dot{x}_{A} = (\underline{A}_{A} - \underline{B}_{A}\underline{K}_{A})\underline{x}_{A} + \underline{B}_{A}\underline{S}_{A}\underline{w}_{A}}{\underline{y}_{A} = \underline{C}_{A}\underline{x}_{A}}$$
(64)

with the pilot control matrix:

5

10

15

20

25

30

35

50

55

$$S_{A} = \begin{bmatrix} K_{VA0} & K_{VA1} & K_{VA2} \end{bmatrix} \tag{65}$$

and the pilot control gains K_{VD0} to K_{VD2} , to be calculated. After evaluating Equ. 65, the output voltage of the pilot control block 91 is given by:

$$u_{AVorst} = K_{VA0}\dot{\phi}_{Aref} + K_{VA1}\ddot{\phi}_{Aref} + K_{VA2}\ddot{\phi}_{Aref}$$
 (66)

[0105] The calculation of the individual pilot control coefficients is carried out in the same way as described in Equ. 38 - 40 for the rotation axis controller.

[0106] The pilot control gains are, in turn, available depending on the elements of the mass matrix, the damping matrix, the stiffness matrix and further model parameters. The corresponding matrix elements are dependent on further characteristics, such as the angle of elevation, the articulation angle, the run-out length etc. If these parameters change, then the pilot control gains also change automatically, so that the vibration damping behaviour of the pilot control is maintained while moving the cage. Furthermore, in the pilot control gains for elevation, a dependency of the pilot control coefficients upon the control gains k_{1A} to k_{3A} can be identified, as already in the rotation axis controller.

[0107] The derivation of these feedback coefficients is explained in the following section of the description of the invention.

[0108] The control feedback 93 is implemented as a state controller. The individual feedback gains are calculated analogue to the rotation axis controller (Equ. 42 - 48). The components of the state vector \underline{x}_A are weighted with the control gains k_{iA} of the control matrix \underline{K}_A and fed back to the servo input control system.

[0109] The eigen-values of the system can be selectively displaced by feeding back the state variables via the control matrix \underline{K}_A to the control input, as the position of the eigen-values is in turn determined by the analysis of the following determinants:

$$\det(sI - A_A + B_A \cdot K_A) \equiv 0 \tag{68}$$

[0110] The analysis of Equ. 68 leads to a 3^{rd} order polynomial which is again dependent on the control gains k_{iA} (i=1.. 3). The characteristic equation of the controlled system then becomes:

$$s^{3} + a_{2}(k_{3A}, k_{1A})s^{2} + a_{1}(k_{2A}, k_{1A})s + a_{0} \equiv 0$$
 (69)

[0111] The zeros of Equ. 45 (and thus the dynamics of the closed-loop system) can again be influenced by the control gains k_{iA} . The position of the poles is known from the calculation of the open-loop poles. There exists a negative real pole (conditional on the time delay constant of the hydraulics from Equ. 52) and one conjugated complex pole pair conditional upon the vertical bending. With this a priori knowledge, the following structure of the pole specifying polynomial results:

$$p_{A}(s) = (s - p_{h}) \cdot (s - (p_{v,r} + i \cdot p_{v,im})) \cdot (s - (p_{v,r} - i \cdot p_{v,im}))$$
(70)

p_h Hydraulic pole

5

20

25

30

35

40

50

 $p_{V_z,r}$ Real part bending pole

 $p_{V_{\tau},im}$ Imaginary part bending pole

[0112] Access to the conjugated complex pole pair again takes place in direct manner on the real and imaginary parts. In this way one can selectively influence the vibration and damping for the vertical bending of the arm by adjustment of the controller. As with the rotational axis controller, the control coefficients are functions of the real and imaginary parts of the conjugated complex pole pair.

[0113] The pole positions, according to Equ. 70, are to be chosen so that the system is stable, the controller works adequately fast with good damping and the limit of the variables is not reached under the typically arising control deviations. The exact values can be established before initial operation via simulation according to these criteria.

[0114] As with the axis of rotation, the control gains can be determined by comparing coefficients of the polynomials analogue to Equ. 47

$$\det(s\underline{I} - \underline{A}_A + \underline{B}_A \cdot \underline{K}_A) \equiv p_A(s) \tag{71}$$

[0115] Based on Equ. 71, there results a set of linear differential equations to be solved dependent on the control gains k_{iA} , as with the axis of rotation. The analysis of this set of equations produces analytic expressions for the respective control gains dependent upon the desired poles from Equ. 70 and the individual system parameters. If these parameters change, as for example the angle of articulation or the run-out length, then these changes are immediately taken into account by a variation of the individual control parameters.

[0116] With feedback of $\dot{\phi}_A$, v_z , \dot{v}_z , the output of the state controller block 93 is then

$$u_{Artick} = k_{1A}\dot{\varphi}_A + k_{2A}v_z + k_{3A}\dot{v}_z \tag{73}$$

[0117] Taking into account the pilot control 91, the reference control voltage of the proportional valve for the axis of elevation/inclination is then

$$u_{Aref} = u_{Avorst} - u_{Ar\curl{u}ck} \tag{74}$$

[0118] The states φ_A, ν_z, ν̄_z of the subsystem elevation under consideration are measured either directly or indirectly by suitable sensors. The elevation velocity is usually measured on the ladder hinge with corresponding encoders. If strain gauges (SG) are used as measurement pick-up sensors for the elastic degrees of freedom, it follows to locate these in corresponding positions on the ladder unit. The sensor data is further processed in block 95, measurement data processing. For example, two SGs can be installed right- and left-sided respectively on the lower and upper rails of the ladder in a vertical preferred direction (vertical SG). From this results

$$v_{z} = b_{\varepsilon v} \frac{-\left(\varepsilon_{vr} + \varepsilon_{vl}\right)/2 \cdot l_{A}^{3}}{\left(l_{A} - l_{0v}\right)} \tag{75}$$

with

5

10

20

25

30

45

50

 ε_{v} - Strain at SG position

 I_{0v} - SG position (distance from the fixing point in the x direction)

b_{sy} - proportionality factor

[0119] Only the dynamic signal portions of the bending are relevant for the control. Steady-state signal portions come about through the gravitational force of the ladder and through possibly existing offset portions of the SG signal and must be filtered out reliably. For compensation, a high pass filter can be used in combination with an upstream gravitational compensation.

$$v_{z}' = b_{\varepsilon v} \frac{-\left(\left(\varepsilon_{vr} + \varepsilon_{vl}\right)/2 - \varepsilon_{offs}\right) \cdot l_{A}^{3}}{\left(l_{A} - l_{0v}\right)} - \frac{-m_{ers}g\cos\varphi_{A}}{c_{v}(l_{A})}$$
(76)

with

5

10

 v_z' - vertical displacement at reference point articulated joint after gravitational compensation ϵ_{offs} -SG-Offset (ϵ_{offs} = -69.65 μ m/m)

[0120] The parameter $\varepsilon_{\text{offs}}$ can be determined from a series of measurements with slowly varying ladder run-out length. [0121] The corresponding time derivatives of the decoupled bending states can be implemented with the aid of suitable real differentiator modules.

[0122] As there exists a system with locally distributed parameters, higher harmonics also occur in the subsystem elevation. These are correspondingly recorded by the sensor elements and coupled in the signal flow of the control feedback. The control behaviour is thus negatively influenced. On the other hand, it can happen that the measurement signal of the vertical bending has an offset, or the gravitational compensation does not present a sufficiently robust performance. This can lead to a non-damped raising motion. In order to solve this problem, the processing of measured data can be supplemented by a disturbance observer with the following functions:

- 1. Correction of offsets on the measured signal owing to gravity and inherent in the measuring principle.
- 2. Elimination of frequency content on the measuring signal, caused by ladder higher harmonics.

25

20

[0123] The vibration differential equation which describes the progression of vibrations of the vertical vibrations to be actively damped, is represented, analogue to Equ. 49e for the axis of rotation, as a damped vibration with an experimentally determined resonant frequency $\overline{\omega}_{vz}$, dependent on angle of elevation, run-out length and articulation angle, and damping \overline{d}_{vz} :

30

$$\ddot{\varphi}_{vz} = -w_{vz}^{2} \cdot \varphi_{vz} - 2d_{vz}w_{vz} \cdot \dot{\varphi}_{vz} \tag{77}$$

35

40

[0124] The angular offset error is assumed to be constant in part.

$$\ddot{arphi}_{o\textit{ffset},vz}$$
 =

 $\ddot{\varphi}_{offset,vz} = 0 \tag{78}$

[0125] In order to eliminate the ladder higher harmonics from the measurement signal, the resonance frequency $\overline{\omega}_{ober,vz}$ and the damping $\overline{d}_{ober,vz}$ are determined experimentally, these being also here generally dependent on the variable system parameters such as ladder length, angles of elevation and articulation and load masses. Alternatively, the resonance frequency and the damping can be determined from a suitable physical model.

50

45

$$\ddot{\varphi}_{ober,vz} = -w_{ober,vz}^{2} \cdot \varphi_{ober,vz} - 2d_{ober,vz} w_{ober,vz} \cdot \dot{\varphi}_{ober,vz}$$
 (79)

[0126] With the state-space representation:

55

$$\underline{\dot{x}}_{vz} = \underline{A}_{vz} \cdot \underline{x}_{vz} + \underline{B}_{vz} \cdot \underline{u}_{vz}
y_{m_{vz}} = \underline{C}_{vz} \cdot \underline{x}_{vz}$$
(80)

State vector:
$$\underline{x}_{vz} = \begin{bmatrix} \varphi_{vz} \\ \dot{\varphi}_{vz} \\ \varphi_{Offset}_{vz} \\ \varphi_{Ober}_{vz} \\ \dot{\varphi}_{Ober}_{vz} \end{bmatrix}$$
Input matrix:
$$\underline{B}_{vz} = \begin{bmatrix} 0 \\ 1 \\ 0 \\ 0 \\ 0 \end{bmatrix}$$

System matrix :

Output matrix:
$$\underline{C}_{vz} = \begin{bmatrix} 1 & 0 & 1 & 1 & 0 \end{bmatrix}$$
 (81)

[0127] According to the invention, the disturbance signal portions are eliminated from the measurement signal with an estimation procedure supported by an observer. The observer equation for a complete observer for the modified state-space model is thus:

$$\hat{\underline{x}}_{vz} = (\underline{A}_{vz} - \underline{H}_{vz}\underline{C}_{vz}) \cdot \underline{x}_{vz} + \underline{B}_{vz} \cdot \underline{u}_{vz} + \underline{H}_{vz}\underline{y}_{mvz}$$
(82)

[0128] The disturbance observer matrix

$$\underline{H}_{vz} = [h_{vz,1}, h_{vz,2}, h_{vz,3}, h_{vz,4}, h_{vz,5}]^T$$

is calculated, for example, according to the Riccati design procedure. It is essential here that the variable parameters such as ladder length, angle of elevation and load masses are likewise taken into account in the observer by adapting

the observer differential equation and the observer gains. The estimated values for φ_{vz} and $\mathring{\varphi}_{vz}$ from the disturbance observer can be fed directly to the state controller. In this way the function of vibration damping can be improved significantly.

[0129] As an alternative to the observer-based elimination of higher harmonics, the feedback gain of the state controller 93 during the raising motion can also be attenuated by means of the proportional attenuator 92. In this way, the control function for the ladder at standstill can be improved if no observer-based elimination has been performed.

[0130] The individual components of the axis controller for the axis of elevation are thereby explained. As a result, the combination of position path planning module and elevation/inclination axis controller fulfils the requirement for a vibration-free and position path-accurate movement of the cage during raising and lowering.

[0131] The axis controllers for extending and retracting the ladder 47, to telescope the articulated arm 413, for the level axis 49 and for the articulated arm 411 are provided with conventional cascade control with an external servo loop for the position and an internal one for the speed, as these axes exhibit only a slight tendency to vibration.

[0132] Therefore a turntable ladder is achieved, the position path control of which allows for position path-accurate travel of the cage with all axes and suppresses active vibrations of the ladder in the process.

Claims

5

15

20

25

30

35

55

- 1. Turntable ladder or the like, with a telescopic ladder unit and, attached at the end of the ladder unit, an articulated arm which carries a cage, which turntable ladder contains a control for moving the ladder sections, formed in such a way that, during cage travel, vibrations of the ladder sections are suppressed, while at least one of the measured variables, bending of the ladder unit in the horizontal and vertical direction, angle of elevation, angle of rotation, runout length and torsion of the ladder unit is fed back via a controller to the control variables for the drives and for which a pilot control is provided which represents the idealised movement behaviour of the ladder during cage travel in a dynamic model, based on differential equations and calculates the idealised control variables for the ladder section drives from the dynamic model for an essentially vibration-free movement of the ladder.
- 2. Turntable ladder according to Claim 1, characterised in that the articulated arm is itself telescopic.
 - 3. Turntable ladder according to Claim 1 or 2, **characterised in that** a position path-planning module is available for the generation of the ladder movement position path in the working area which feeds the movement position path in the form of time functions for the cage position, cage speed, cage acceleration, cage jerking and, if necessary, the derivative of cage jerking to a pilot control block which controls the ladder section drives.
 - **4.** Turntable ladder according to Claim 3, **characterised in that** the position path-planning module allows the input of kinematic restrictions for the time functions cage position, cage speed, cage acceleration and the cage jerking.
- 5. Turntable ladder according to Claim 4, **characterised in that** that the position path-planning module also generates the time function for the derivative of the jerking.
 - **6.** Turntable ladder according to Claim 4 and 5, **characterised in that** the position path-planning module contains steepness limiters to take into account the kinematic restrictions.
- 7. Turntable ladder according to Claim 6, characterised in that the position path-planning module generates continuous jerking functions and from these determines, through integration, the time functions for the cage acceleration, cage speed and cage position.
- **8.** Turntable ladder according to one of the preceding claims, **characterised** through strain gauges as measurement sensors for the bending of the ladder unit in the horizontal and vertical direction and for its torsion.
 - **9.** Turntable ladder according to one of the Claims 1 to 7, **characterised in that** the bending of the ladder unit in the horizontal and vertical direction and its torsion can be reconstructed from the pressure signals of the hydraulic drives of the ladder sections.
 - **10.** Turntable ladder according to one of the preceding claims, **characterised** through a disturbance observer module for correcting the offset of the measurement signals of bending of the ladder unit in the horizontal and vertical

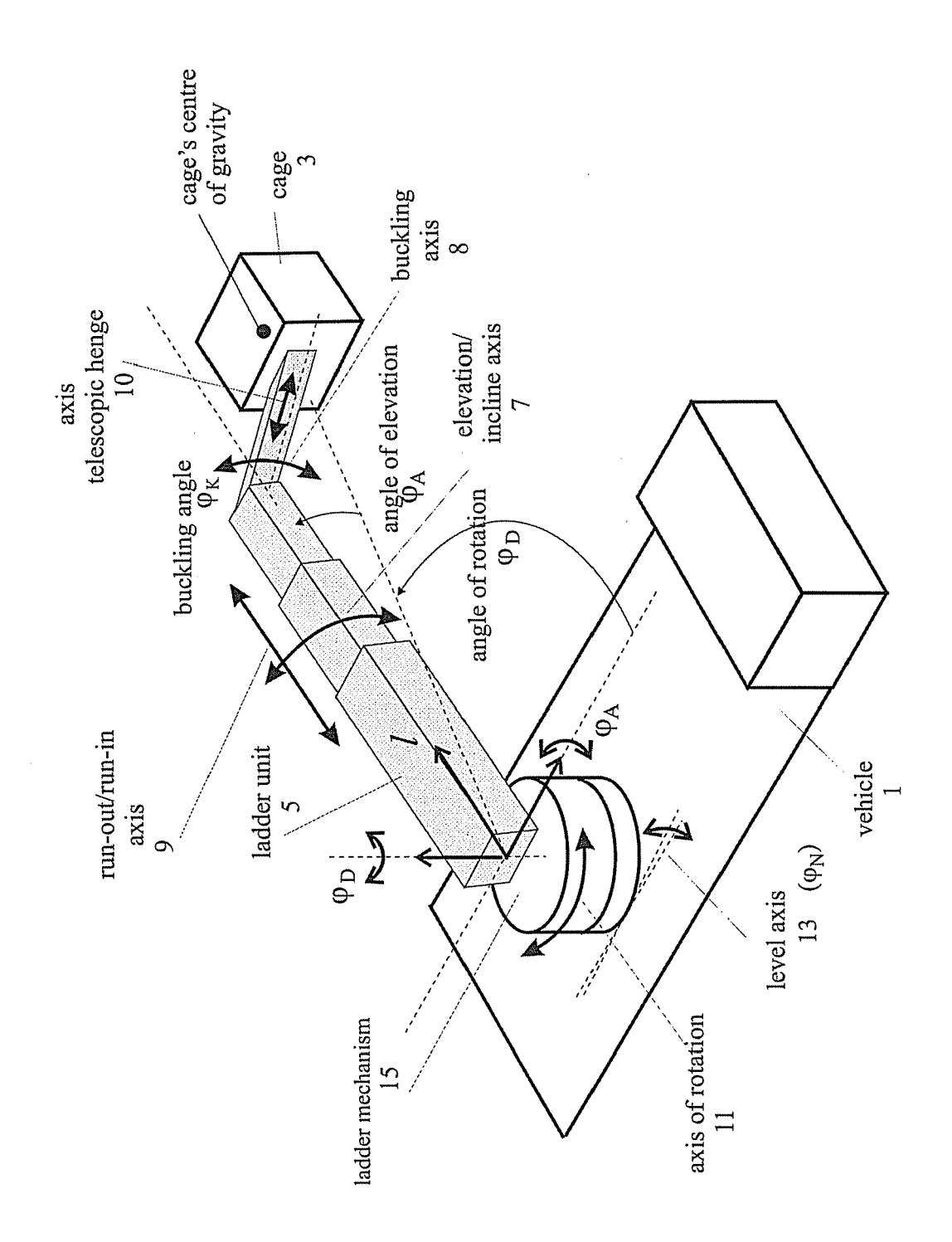
11. Turntable ladder according to one of the preceding claims, characterised in that the controller is designed to weight

5

direction and the torsion and for eliminating the frequency portion of the respective signals which correspond to higher harmonics of the ladder unit.

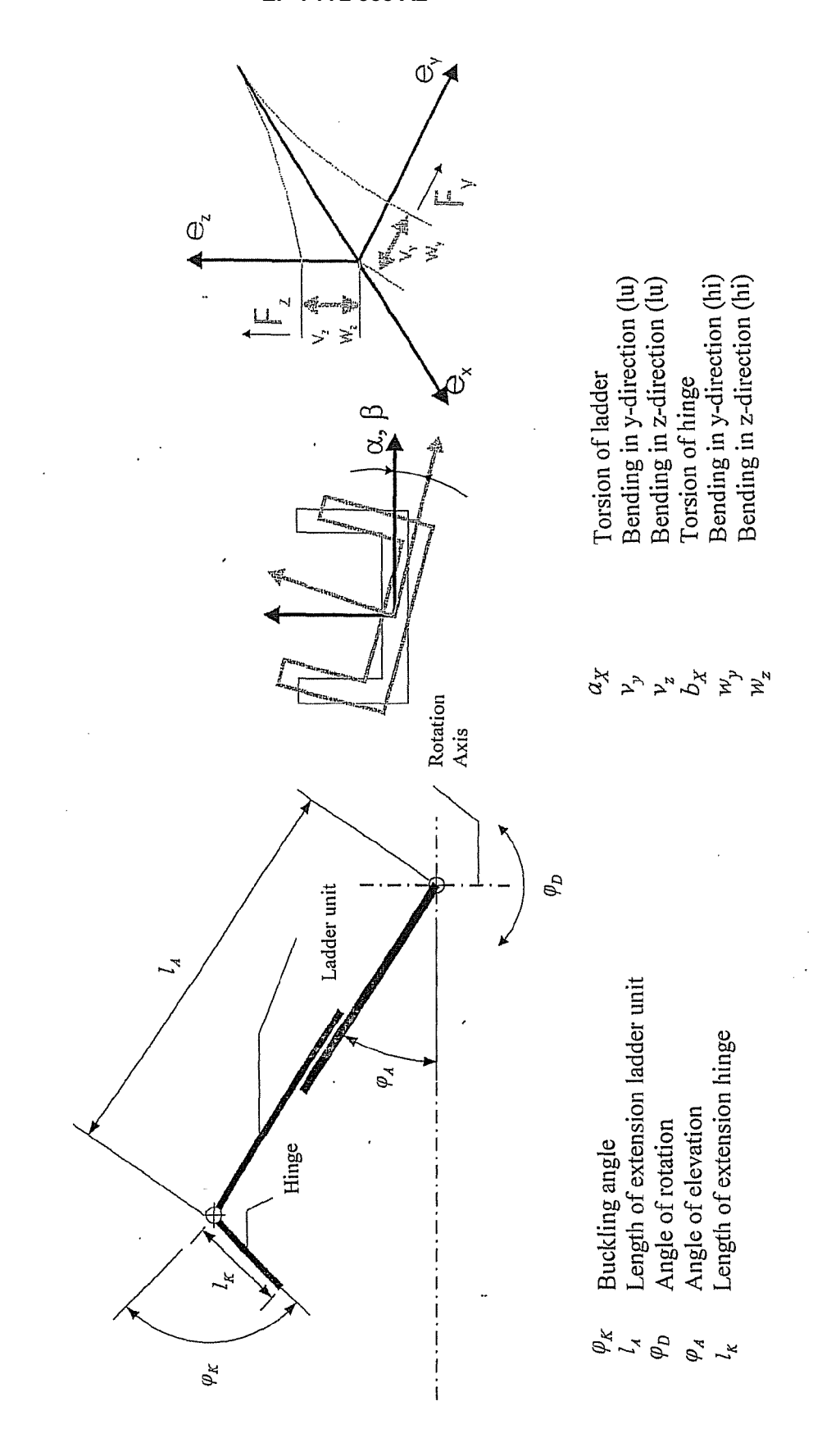
the fed-back measurement values with a control gain and to reduce the control gain for eliminating ladder unit higher

	narmonics.	
10		
15		
20		
25		
30		
35		
40		
45		
50		
55		



Elastic Degrees of Freedom

Inelastic Degrees of Freedom



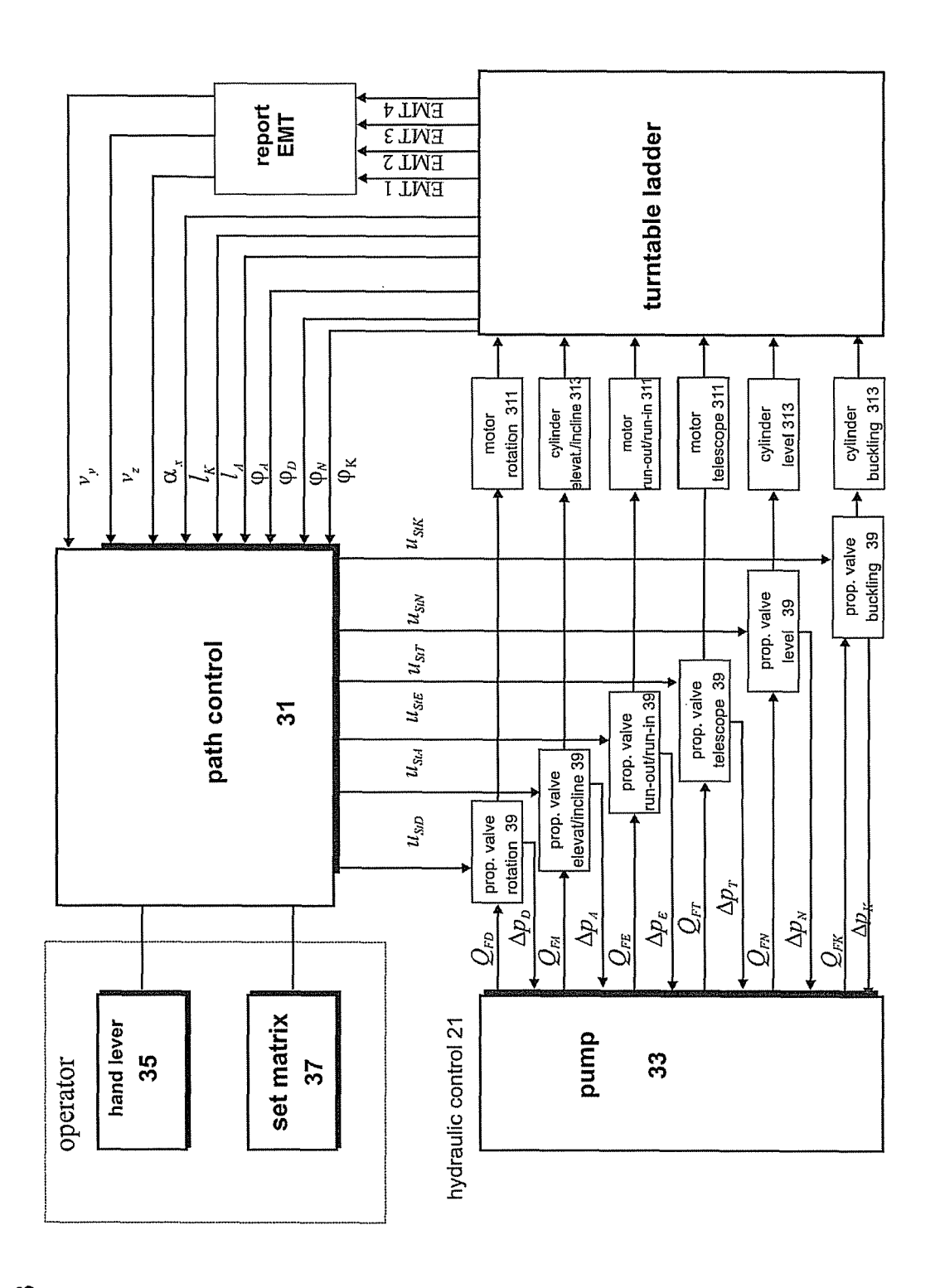
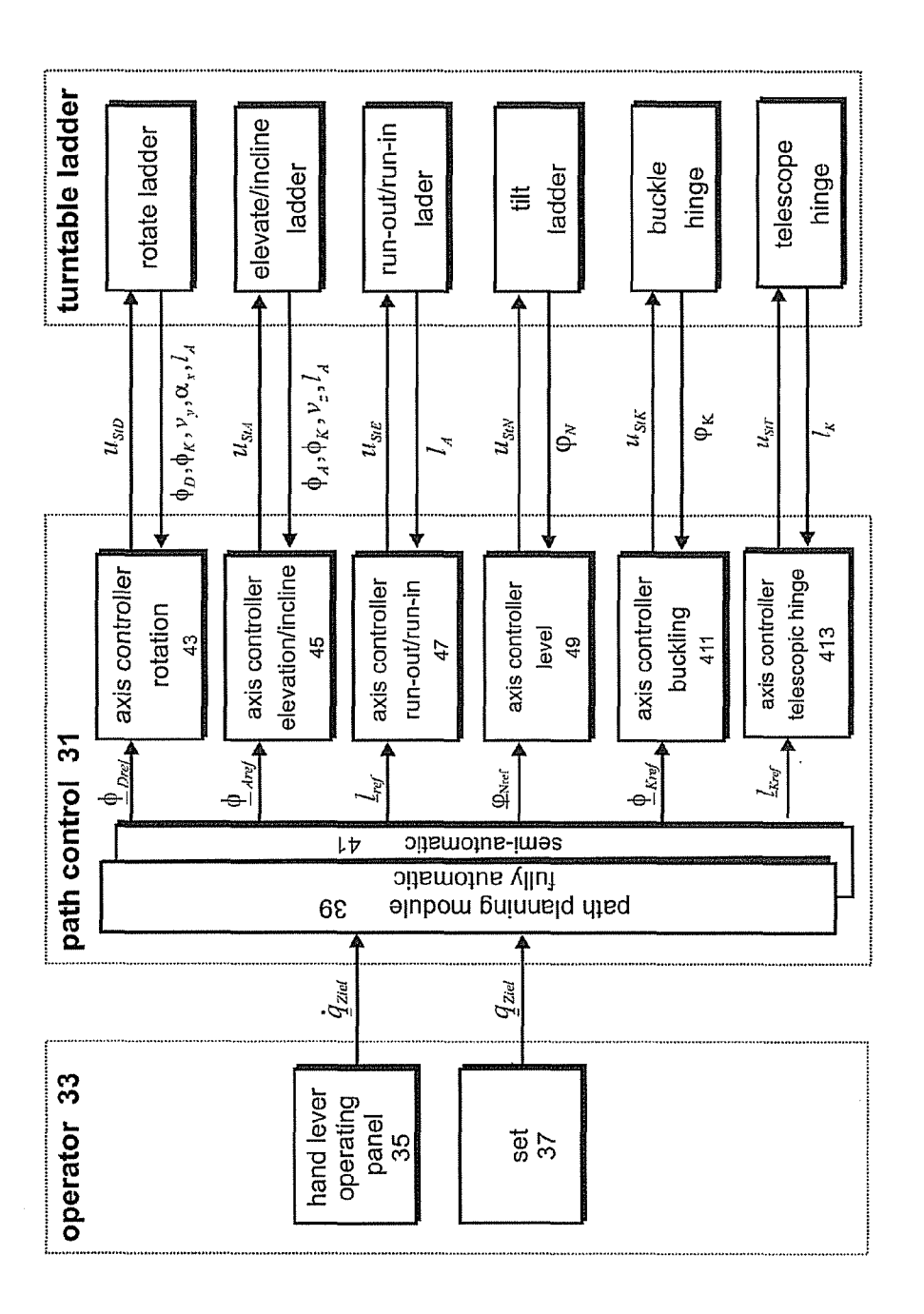
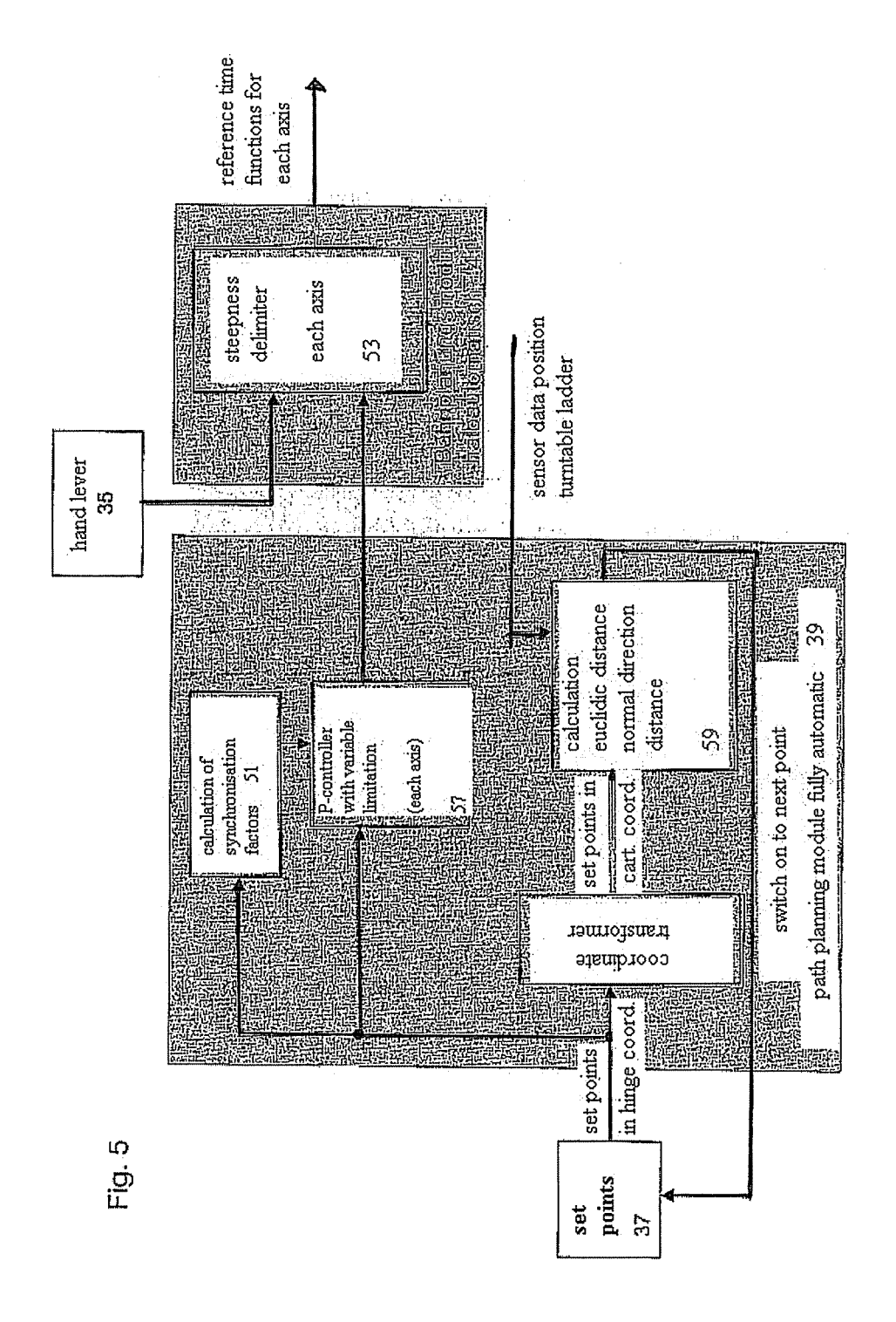
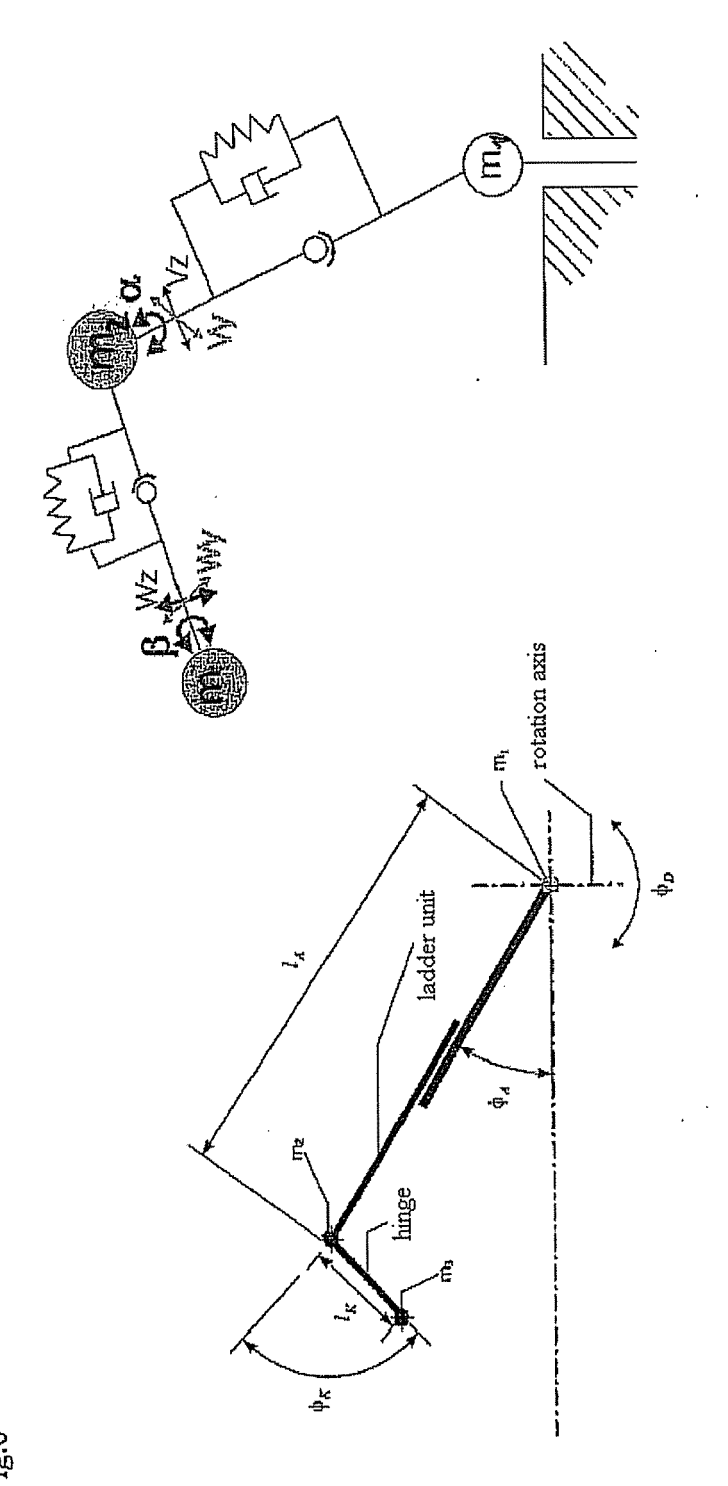


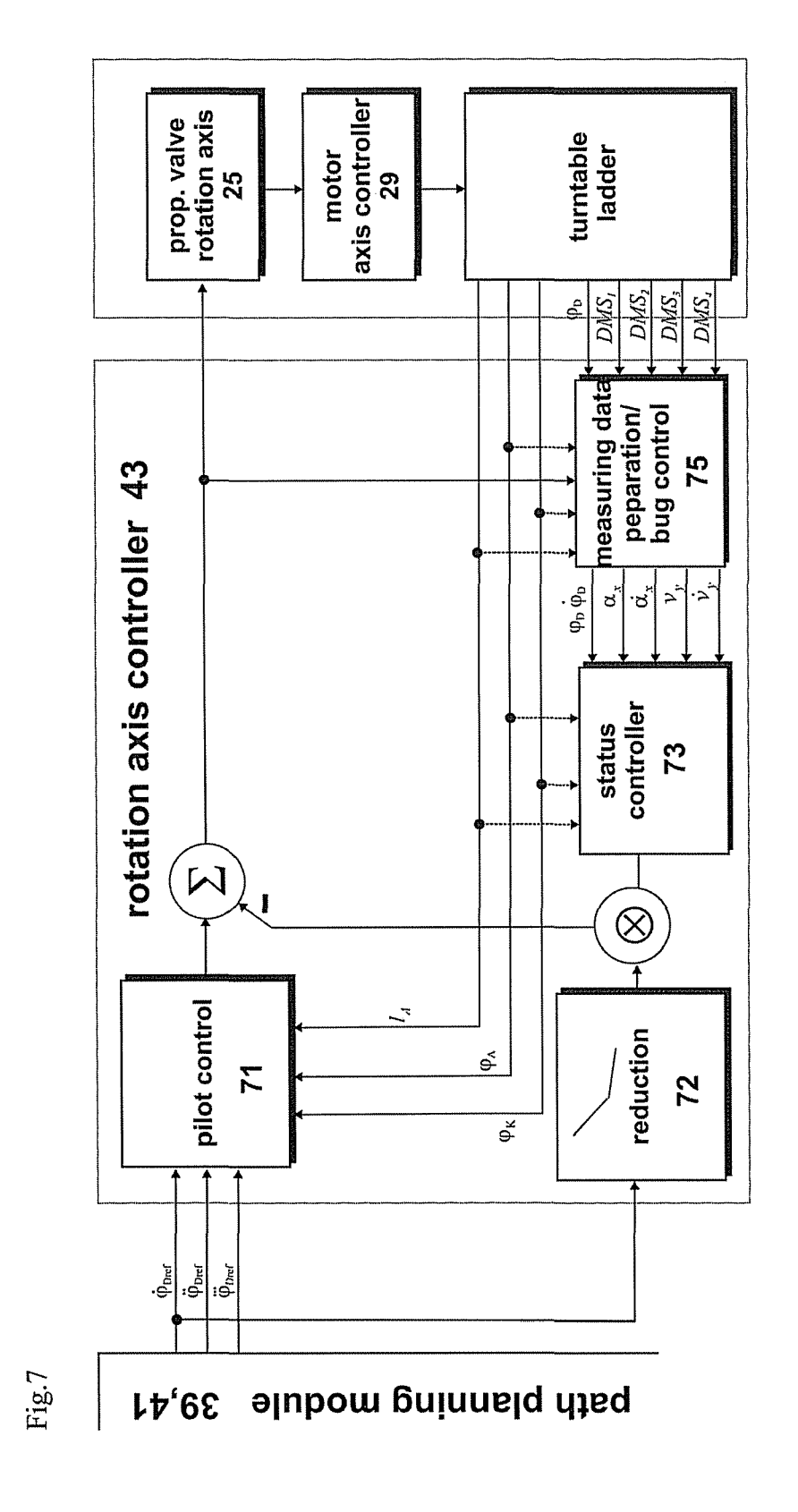
Fig.3

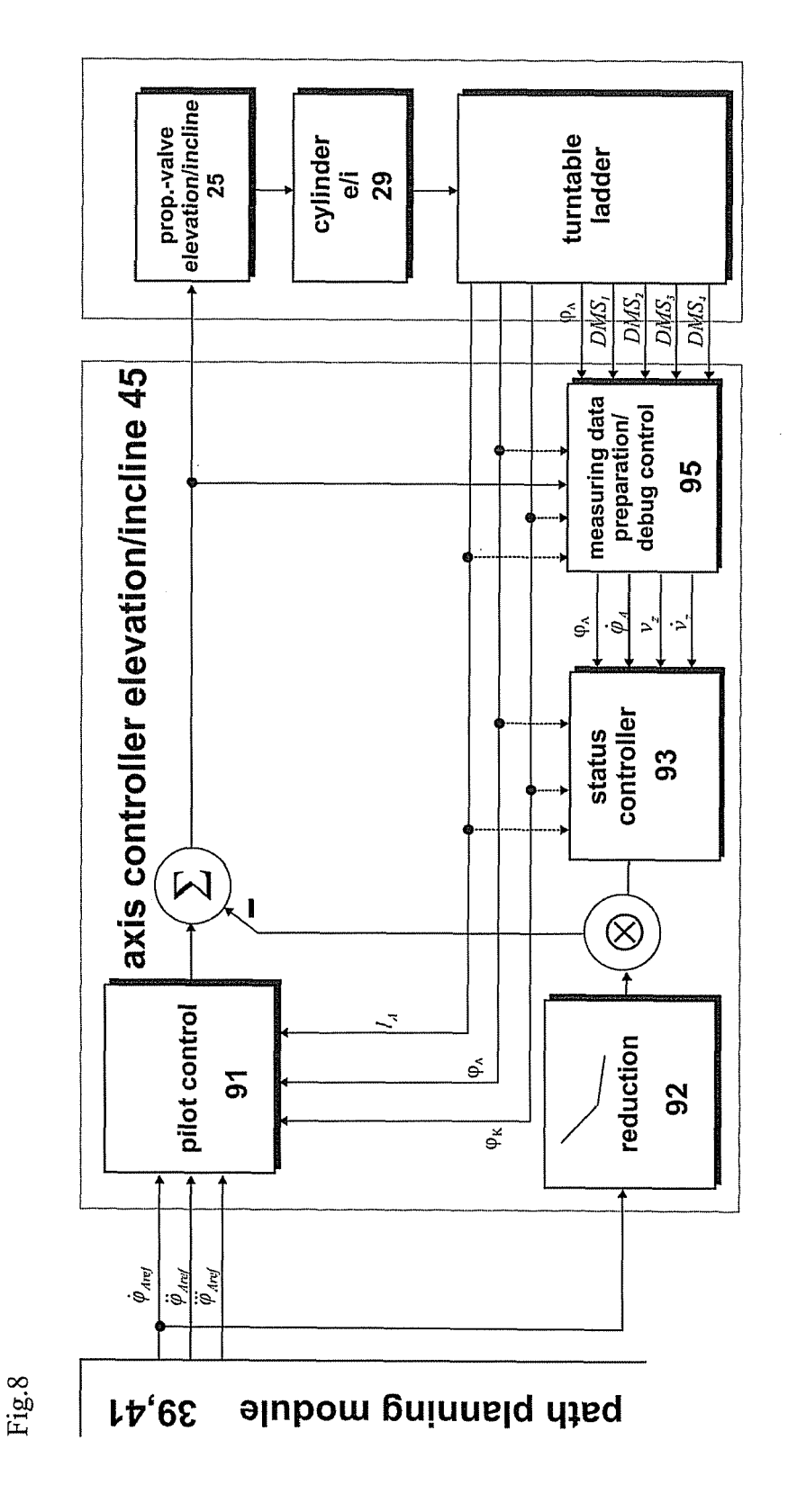


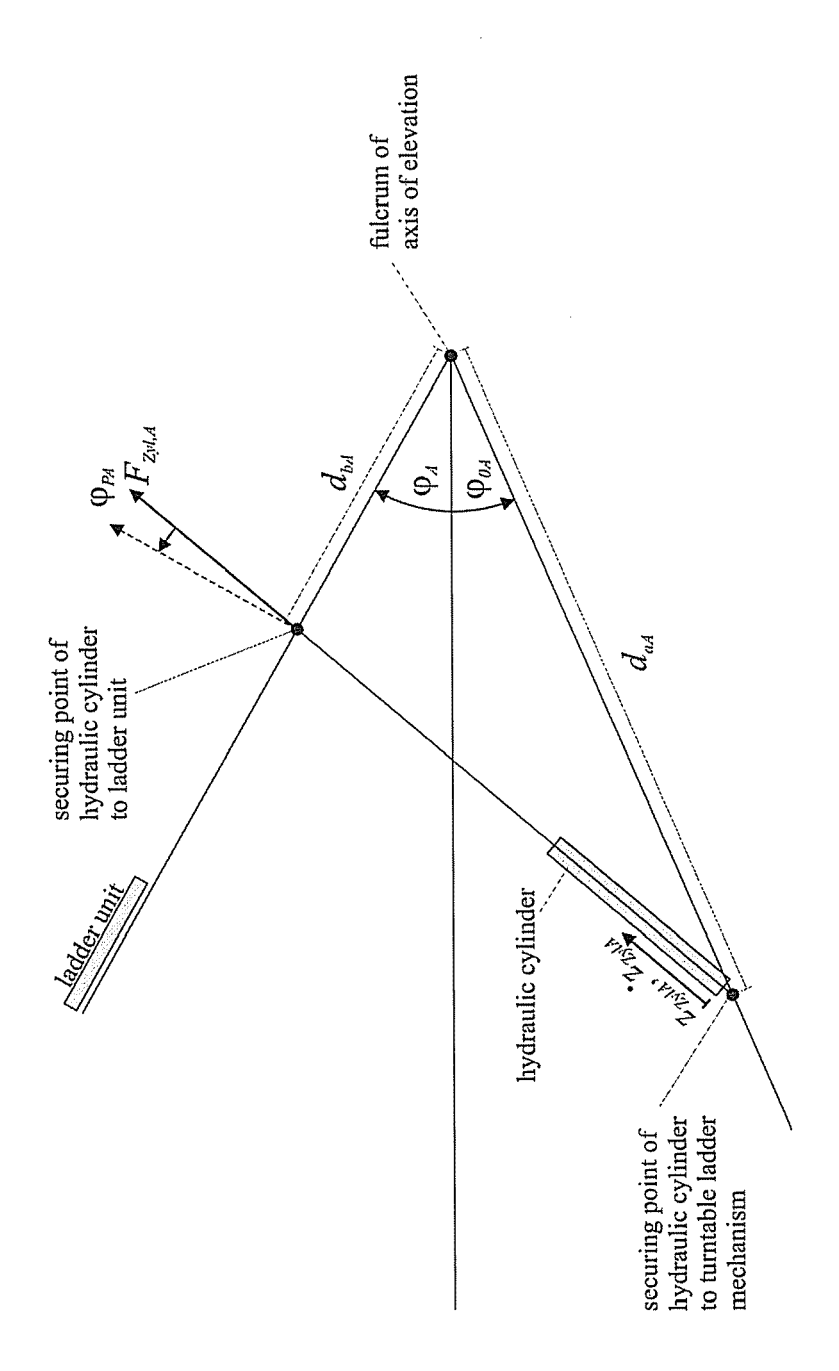




<u>|-</u>----|







REFERENCES CITED IN THE DESCRIPTION

This list of references cited by the applicant is for the reader's convenience only. It does not form part of the European patent document. Even though great care has been taken in compiling the references, errors or omissions cannot be excluded and the EPO disclaims all liability in this regard.

Patent documents cited in the description

• DE 10016136 C2 [0003] [0003]

• DE 10016137 C2 [0003]